Differential lactate and cholesterol synthetic activities in XY and XX Sertoli cells

宍戸, 祐里菜

https://doi.org/10.15017/1806844

出版情報：九州大学, 2016, 博士（理学）, 課程博士
バージョン：

Differential lactate and cholesterol synthetic activities in XY and XX Sertoli cells

Yurina Shishido

Division of System Life Science

Graduate School of Systems Life Science

Kyushu University

Table of Contents

LIST OF SUPPLEMENTAL TABLES

SUMMARY

SRY, a sex-determining gene, induces testis development in chromosomally female (XX) individuals. However, mouse XX Sertoli cells carrying *Sry* (XX/*Sry* Sertoli cells) are incapable of fully supporting germ cell development, even when the karyotype of the germ cells is XY. While it has therefore been assumed that XX/*Sry* Sertoli cells are not functionally equivalent to XY Sertoli cells, it has remained unclear which specific functions are affected. To elucidate the functional difference, I compared the gene expression of XY and XX/*Sry* Sertoli cells. Lactate and cholesterol metabolisms, essential for nursing the developing germ cells, were down-regulated in XX/*Sry* cells, which appears to be caused at least in part by the differential expression of histone modification enzymes SMCX/SMCY (H3K4me3 demethylase) and UTX/UTY (H3K27me3 demethylase) encoded by the sex chromosomes. I suggest that down-regulation of lactate and cholesterol metabolism that may be due to altered epigenetic modification affects the nursing functions of XX/*Sry* Sertoli cells.

INTRODUCTION

In mammals, the *SRY* gene (the sex determining region on the Y chromosome) has generally been thought to be sufficient for differentiation of the testes[1-3]. Indeed, an *Sry* transgene successfully induced testis development in XX fetuses; testicular cords were organized, Sertoli cells were differentiated within the cords, and Leydig cells were present in the interstitial space[4]. However, XX mice carrying an *Sry* transgene (XX/*Sry*) were found to be infertile[5,6]. Phenotypically, spermatogonial cells disappear from the testes soon after birth, and the presence of double X chromosomes has been suggested as a cause[7]. Moreover, since genes essential for spermatogenesis are localized on the Y chromosome[8], XX germ cells are incapable of differentiating into matured male germ cells. The infertility of XX/*Sry* males has therefore been discussed from the viewpoint of a functional deficit of germ cells. It has, however, remained largely unclear whether XX/*Sry* Sertoli cells exhibit functions equivalent to XY Sertoli cells. Ishii *et al*[6] reported the interesting experimental observation that XY germ cells implanted into XX/*Sry* testes differentiated into round spermatids but rarely elongated spermatids. The authors concluded that the milieu established by XX/*Sry* Sertoli cells is insufficient for differentiation into elongated spermatids. However, the specific functions that have been affected in XX/*Sry* Sertoli cells still await clarification.

Since blood vessels are localized in the interstitial space outside the seminiferous tubules and Sertoli cells create a tight blood-testis barrier, nutrients and fuels for energy production cannot be supplied to germ cells via the blood. The Sertoli cells, often referred to as nursing cells, are responsible for the supply of energy and nutrients to the germ cells, with which they remain in close contact throughout the entire differentiation process[9]. Similar to nutrients, oxygen supply is restricted in the

seminiferous tubule, and the testis has therefore been described as an oxygen-deprived organ[10]. In this unusual milieu, spermatocytes and mature sperms prefer lactate as fuel to produce ATP[11]. Sertoli cells produce lactate via glycolysis and then supply it to developing germ cells[12,13].

Another fundamental material supplied to germ cells by Sertoli cells is cholesterol[14]. Sertoli cells are capable of synthesizing cholesterol by themselves, as well as absorbing it from high density lipoprotein (HDL)[15,16]. They also continuously phagocytose developing germ cells as another source of cholesterol[17]. Consequently, the quantity of intracellular cholesterol/cholesterol ester is regulated by the balance of synthesis, influx via the two above-mentioned routes, and efflux. It has been suggested that ATP-binding cassette transporter 1 (ABCA1) mediates cholesterol efflux from Sertoli cells, since disruption of *Abca1* gene led to defects in spermatogenesis together with unusual accumulation of lipids in the Sertoli cells[18]. In addition, gene knockout of retinoid X receptor β (Rxrb, Nr2b2)[19] and double knockout of liver X receptor α/β (Lxrα, Nr1h3 and Lxrβ, Nr1h2)[20] resulted in defects similar to *Abca1* gene knockout, possibly through down-regulation of *Abca1* gene transcription.

Sex chromosomes carry genes encoding histone modification enzymes such as SMCX (KDM5C)/SMXY (KDM5D) and UTX (KDM6A)/UTY. Both SMCX and SMCY mediate the demethylation of histone H3 trimethylated Lysine 4 (H3K4me3)[21]. UTX mediates the demethylation of histone 3 trimethylated Lysine 27 (H3K27me3), whereas such activity has not been found for UTY[22,23]. Evidence from multiple sources indicates that H3K4me3 accumulates predominantly around the transcription start sites of active genes, while H3K27me3 is distributed throughout gene bodies with inactive transcription[24-26]. The physiological function of *Utx* has been

investigated using gene knockout mice[27-29]. Interestingly, in addition to affecting morphology, *Utx* was found to be required for sexually dimorphic deposits of H3K27me3[29].

In the present study, I investigated the functional differences between XY and XX/*Sry* Sertoli cells by focusing on their role as nursing cells.

MATERIALS AND METHODS

Mice

A line of XX sex-reversed mice was established using an *Sry* transgene driven by the basal promoter of the *Hsp70.3* gene[30]. The presence of the transgene in mice was confirmed by PCR with primers for *Sry* (Supplemental Table S1). Genetic sex (XY or XX) was determined by PCR using the primers for *Ube1*. Sox9-EGFP knock-in mice have been reported previously[31]. To label XX/*Sry* Sertoli cells with EGFP, XX/*Sry* mice were mated with Sox9-EGFP mice. All protocols for the animal experiments were approved by the Animal Care and Use Committee of Kyushu University. All experiments were performed in accordance with the guidelines.

Immunofluorescence microscopy

Frozen sections prepared from testes were used for immunostaining[32]. Anti-EGFP rat monoclonal antibody (1:1000; Nacalai Tesque, Kyoto, Japan) and anti-SOX9 rabbit antiserum[33] (1:2000) were used as the primary antibodies, and ALEXA Fluor 488 goat anti-rat IgG and ALEXA Fluor 555 goat anti-rabbit IgG (1:500; Thermo Fisher Scientific, Waltham, MA, USA) were used as the secondary antibodies. DAPI (4′6′-diamidino-2-phenylindole) was used for nuclear staining. The specimens were observed using a BZ-9000 microscope (Keyence, Osaka, Japan).

Preparation and culture of Sertoli cells

Testes at postnatal days 1 and 21 (P1 and P21) were incubated in Earle's balanced salt solution (Sigma, St. Louis, MO, USA) containing 1 mg/ml collagenase (Thermo Fisher Scientific), 0.5 mg/ml dispase (Thermo Fisher Scientific) and 2.5 mg/ml trypsin (Sigma) at 34 ºC for 30 min, and following the addition of

0.3 mg/ml deoxyribonuclease I (Roche, Basel, Switzerland), were incubated for another 30 min at 34 ºC. After centrifugation, the cells were suspended in PBS with 7-amino-actinomycin D (7AAD; BD Bioscience, Franklin Lakes, NJ, USA). The cells were washed with PBS containing 0.3 mg/ml deoxyribonuclease I, and filtered using a 70 μm cell strainer (BD Bioscience). EGFP-positive Sertoli cells were isolated by fluorescence-activated cell sorting (FACS) using a JSAN cell sorter (Bay bioscience, Kobe, Japan). For siRNA treatment, Sertoli cells at P21 were cultured at 34 ºC on 24-well culture plates (Asahi Glass, Tokyo, Japan) pre-coated with collagen type I (Cell Matrix I-C; Nitta Gelatin, Osaka, Japan) in DMEM/Ham's F-12 (1:1; Nacalai Tesque) supplemented with 10% FBS and Penicillin-streptomycin-glutamine (Thermo Fisher Scientific).

siRNA treatment

Using an RNeasy Mini or Micro kit (Qiagen, Hilden, Germany), total RNA was prepared from XY and XX/*Sry* Sertoli cells, and XY Sertoli cells were treated with siRNA duplex (stealth RNAi™; Srebf2-MSS277288 or Negative Control Medium GC Duplex; Thermo Fisher Scientific) using Lipofectamine RNAiMAX reagent (Thermo Fisher Scientific) for 48 h.

Quantitative RT-PCR (qRT-PCR)

Total RNAs were prepared from Sertoli cells at P1 and P21, and from testes and ovaries at P21. They were subjected to cDNA synthesis using M-MLV reverse transcriptase (Thermo Fisher Scientific), and then to qRT-PCR using SYBR Select Master Mix (Thermo Fisher Scientific) and the CFX96 Touch Real-Time PCR Detection System (Bio-Rad Laboratories, Hercules, CA, USA). The primers used for

qRT-PCR are listed in Supplemental Table S8. Listed values were standardized using β-actin (*Actb*) or 18s ribosomal RNA (*Rn18s*). RT-PCR was performed in biological triplicate. Data are presented as means ± 1 standard deviation (SD). Differences between experimental groups were tested for significance using a two-tailed Student's *t*-test.

mRNA sequencing and data analyses

Poly(A)$^+$ RNAs were prepared from XY and XX/*Sry* Sertoli cells using oligo (dT) magnetic beads. Preparation of mRNA-seq library and subsequent sequencing was carried out as described previously[34]. Mapping and quantification of gene expression was performed by Tophat[35], version 2.0.8, and RSEM[36], version 1.2.11, respectively. Expression levels of genes were represented using the number of fragments per kilobase of transcript per million fragments mapped[37] (FPKM). Fold change in FPKM values in XX/*Sry* Sertoli cells relative to XY Sertoli cells was calculated. Gene sets were subjected to gene ontology[38] (GO) and KEGG pathway analyses using DAVID[39]. mRNA-seq data have been deposited in DDBJ/EMBL/GeneBank under accession code DRA004090.

Immunoblot analysis

Whole cell lysates were prepared from XY and XX/*Sry* Sertoli cells using lysis buffer (50 mM Tris-HCl pH 8.0, 50 mM NaCl, 1 mM EDTA, and 1% Sodium Dodecyl Sulfate (SDS)). After the protein concentration was determined using a BCA™ Protein Assay Kit (Pierce Biotechnology, Rockford, IL), 10 μg of the whole cell lysates were subjected to SDS-polyacrylamide gel electrophoresis, followed by immunoblotting. Anti-LDHA (Cell Signaling Technology, Danvers, MA, 1:1000),

anti-HMGCR (Abcam, Cambridge, MA, 1:1000), anti-CYP51 (1:1000)[40], or anti-α-tubulin antibody (T-9026, Sigma-Aldrich, St. Louis, MO, 1:1000) was used as the primary antibodies. Anti-rabbit donkey IgG (1:1000) and anti-mouse donkey IgG (GE Healthcare, Piscataway, NJ, 1:1000) were used as the secondary antibodies. Bound antibodies were detected using the Chemi-Lumi One L Western Blotting Detection System (Nacalai Tesque, Kyoto, Japan).

Chromatin immunoprecipitation-sequence (ChIP-seq)

A total of 10^6 Sertoli cells fixed by formaldehyde (0.5%, 5 min at room temperature) were lysed with 600 μl Lysis Buffer (5 mM HEPES (pH 8.0), 200 mM KCl, 1 mM $CaCl_2$, 1.5 mM $MgCl_2$, 5% Sucrose, 0.5% Triton X-100), and then sonicated (5 × 15-s pulses with 59-s break intervals) using the Bioruptor plus sonication device (Diagenode, Denville, NJ, USA). Samples were then digested with 100 U/ml micrococcal nuclease (MNase; Takara Bio, Shiga, Japan) at 37 ºC for 1 h to shear the chromatin. MNase digestion was terminated by the addition of 5 mM EDTA (pH 8.0). The sheared chromatin fraction was centrifuged at 15,000 × *g* for 10 min to remove insoluble materials. Supernatant was then incubated overnight at 4 ºC with magnetic beads (Dynabeads Protein A; Veritas, Tokyo, Japan) pre-bound with a mouse monoclonal antibody against H3K4me3 or H3K27me3. The beads were washed with Lysis Buffer, Wash Buffer 2 (5 mM HEPES (pH 8.0), 500 mM KCl, 1 mM $CaCl_2$, 5% Sucrose, 0.5% NP-40), and Wash Buffer 3 (10 mM Tris-HCl (pH 8.0), 1 mM EDTA (pH 8.0)). Finally, chromatin fractions (ChIP fractions) were eluted from the beads with 50 mM Tris-HCl (pH 8.0), 10 mM EDTA (pH 8.0), and 1% SDS. After crosslinking was reverted by heating at 65 ºC for 16 h, DNA fragments were purified using QIAquick PCR Purification kit (Qiagen), and used to prepare a ChIP-

seq library with TruSeq ChIP Sample Preparation Kit (Illumina, San Diego, CA, USA). Adaptor-ligated DNA fragments 250 bp in length were recovered. The ChIP-seq library was subjected to sequencing with a HiSeq 2000 (Illumina). Total DNA fragments prepared from the shared chromatin fraction (input fraction) were sequenced as the control. ChIP-seq data have been deposited in DDBJ/EMBL/GeneBank under the accession code DRA004110.

Analysis of ChIP-seq data sets

ChIP-seq reads were aligned to the reference mouse genome (mm10) using Bowtie[41], version 1.0.0. The multiple-hit reads were excluded, and only the uniquely mapped reads to the reference mouse genome were kept for further analysis. The number of ChIP-seq reads for H3K4me3 mapped around the transcription start site (TSS; 2 kb upstream to 2 kb downstream) was counted using BEDTools[42], version 2.17.0. For the analysis of H3K27me3, the number of reads mapped from 2 kb upstream of the TSS to the transcription termination site (TTS) was counted. The number of reads was normalized by the total number of mapped reads to obtain RPM (reads per million). Enrichment values for H3K4me3 and H3K27me3 were defined for each gene as the ratio of RPM in the ChIP fraction to that in the input fraction. Read density profiles of H3K4me3 and H3K27me3 were generated as described previously[43].

Measurement of metabolites

Sertoli cells (5×10^5) at P21 were cultured for 3 days. The lactate concentration of 30 μl of the medium was determined at 6 and 24 h after medium change using the Lactate Assay Kit (BioVision, Milpitas, CA, USA). To determine cholesterol

synthetic activity, Sertoli cells (1 x 10^6) were incubated in a serum-free medium containing [1,2-^{14}C]-acetate (PerkinElmer, Inc., Boston, MA USA), 50 μM aminoglutethimide (Sigma) and 2 μg/ml 58-035 (ACAT2; acyl-CoA cholesterol acyltransferase inhibitor; Sigma) for 2.5 or 3 h at 34 ºC. All lipids, including cholesterol, were extracted using chloroform/methanol (2:1, v/v), then separated by thin-layer chromatography on silica gel with benzene-ethylacetate (2:3, v/v) as a solvent. The radioactivity of a spot containing free and esterified cholesterol visualized with iodine vapor was determined by liquid scintillation counting. The extent of [1,2-^{14}C]-acetate incorporation into the cholesterol was expressed as cpm/μmol acetate/h.

Measurement of quantities of cholesterol and cholesterol precursors

Sertoli cells (3 x 10^4) were suspended in 0.2 ml methanol and sonicated (2 × 20-s pulses with 30-s break intervals) using Bioruptor Plus (Diagenode), then centrifuged for 5 min at 15,000 rpm to exclude methanol-insoluble cellular components. The supernatant (methanol-soluble fraction) was recovered and evaporated to remove the methanol. Gas chromatography-mass spectrometry analysis (GC-MS) was performed using an Agilent 6890 Plus gas chromatograph interfaced with a single-quadrupole Agilent 5975C MSD (Agilent Technologies, Palo Alto, CA, USA) as previously described[44].

Determination of testosterone, FSH, and LH concentrations

Blood plasma samples collected individually from 6 XY and 6 XX/*Sry* mice at P21 were subjected to LC-MS/MS analysis to determine testosterone concentration. The measurement was performed according to a previous report[45]. Briefly, plasma

samples were spiked with $^{13}C_3$-testosterone and extracted with 1 mL of 90% hexane/10% ethyl acetate (v/v). After evaporation, the samples were reconstituted in 90% methanol/10% H_2O (v/v) for LC-MS/ MS analysis. The samples were analyzed on a QTRAP 5500 LC-MS/MS system (AB SCIEX, Framingham, MA) connected to a Shimadzu LC 20A HPLC system. For determination of FSH and LH concentration, blood plasma samples were collected individually from 7 XY and 6 XX/*Sry* mice at P21. Plasma FSH and LH concentrations were determined using Rodent FSH ELISA Test Kits and Rodent LH ELISA Test Kits (Endocrine technologies, Inc., Newark, CA), respectively, according to the manufacturer's instructions.

Statistical analysis

All experiments were performed with at least three biologically independent samples. Data are presented as the mean and standard deviation. The number of the sample is indicated with 'n' in figure legends. The statistical significance was examined using a two-tailed Student's *t*-test.

RESULTS

Preparation of XY and XX/Sry Sertoli cells

To examine the contribution of sex chromosomes to gene expression in Sertoli cells, I used XY wild type and XX transgenic mice carrying the *Sry* transgene (XX/*Sry*). Sertoli cells from these mice were labeled with EGFP as described in 'Materials and Methods'. As expected, all SOX9-positive (SRY-box containing gene 9) Sertoli cells were positive for EGFP in the testes of XX/*Sry* as well as XY wild type mice on postnatal days 1 and 21 (Fig. 1a). As reported previously[5], germ cells had disappeared from the seminiferous tubules of the XX/*Sry* testes by P21. Whole testicular cells prepared from P1 and P21 testes were subjected to FACS. EGFP-positive and -negative cell fractions were recovered (Fig. 1b). Fluorescence microscopy indicated that more than 92% of the cells were EGFP-positive in all preparations (Fig. 1c).

Total RNAs were prepared from P1 and P21 EGFP-positive and -negative cells at and used for qRT-PCR analysis (Fig. 1d). As expected, *Sox9* mRNA was enriched in the EGFP-positive cell fractions, whereas a germ cell marker (homologue of a DEAD (Asp-Glu-Ala-Asp) family gene (*Ddx4*, *VASA*)), and a Leydig cell marker (*Hsd3b1* (*Hydroxysteroid dehydrogenase Type 3b1*)) were enriched in the EGFP-negative cell fractions. Consistent with the disappearance of germ cells from XX/*Sry* testes, expression of *Ddx4* was much reduced in the EGFP-negative cell fraction of XX/*Sry* testes. Up-regulation of *Hsd3b1* in these cells might have resulted from an increased proportion of Leydig cells following the disappearance of the germ cells. Taken together, these marker gene expressions indicate that the EGFP-positive cell fractions prepared from the XY and XX/*Sry* testes comprised predominantly Sertoli cells.

Hormones necessary for reproductive activities were measured in XY and XX/*Sry* mice at P21. As shown in Fig. 1e, plasma testosterone was decreased in XX/*Sry* mice as compared to XY mice. Such significant alteration was not observed in the amounts of follicle stimulating hormone (FSH) or luteinizing hormone (LH). Consistent with the decreased testosterone concentration, the testicular size of XX/*Sry* mice was smaller than that of XY mice (Fig. 1f). Estradiol is a potent estrogen in females, but the concentration is too low to determine precisely in males. Therefore, I determined the expression level of the *Cyp19* gene, which is essential for the synthesis of estradiol. As shown in Fig. 1g, the expression of *Cyp19* in the XX ovary was higher than that in the XY testis. *Cyp19* gene expression was not observed in the XX/*Sry* testes, suggesting that estradiol could not be synthesized in the XX/*Sry* testis.

Gene expression in XY and XX/Sry Sertoli cells

The RNAs prepared from XY and XX/*Sry* Sertoli cells at P1 and P21 were sequenced. As summarized in Supplemental Table S2, approximately 30 million reads were obtained from every sample. More than 97% of reads were mapped to the reference genome, suggesting that the sequence data sets were of sufficient quality for further analyses. Gene expressions were compared between the two types of Sertoli cells at P1 and P21. Correlation coefficients between the cell types were 0.997 at P1 and 0.971 at P21, indicating that the gene expressions of the two types of Sertoli cells were very similar at P1 and differed slightly more at P21 (Fig. 2a). Consistent with this, 38 genes were up-regulated more than 1.5-fold and 86 genes down-regulated less than 1.5-fold in the P1 XX/*Sry* Sertoli cells, and 422 and 834 genes were respectively up- and down-regulated by the same margins in the P21 XX/*Sry* Sertoli cells (Fig. 2b).

Genes displaying differential expression in the P1 XX/*Sry* Sertoli cells are listed in Supplemental Tables S3 and S4. *Sry* and *Xist* (inactive X-specific transcript) were treated as up-regulated genes in the P1 XX/*Sry* Sertoli cells (Supplemental Table S3). In the case of *Sry*, this was because the expression of the exogenous *Sry* gene is driven by *Hsp70.3* basal promoter. The increase of *Xist* suggests that X chromosome inactivation occurs even though the fate of cells carrying two X chromosomes is changed to male supporting Sertoli cells. Four Y-linked genes (*Smcy (Kdm5d), Ddx3y, Eif2s3y*, and *Uba1y*) were recorded as down-regulated in P1 XX/*Sry* Sertoli cells (Supplemental Table S4). This is consistent with the fact that the Y chromosome is absent from XX/*Sry* transgenic mice. Interestingly, the expression of genes for ribosomal protein (*Rpl36*, *Rps29*, *Rplp1*, and *Rps21*) and mitochondrial ribosomal protein (*Mrps12*) was decreased in the XX/*Sry* Sertoli cells.

Genes that were up- or down-regulated in P21 XX/*Sry* Sertoli cells are summarized (data not shown in this thesis). I attempted to extract the biological events/pathways related to the listed genes by conducting GO and KEGG pathway analyses. Results are summarized in Supplemental Tables S5 and S6.

Genes up-regulated in P21 XX/*Sry* Sertoli cells were not distinguished by high fold enrichment and *P*-value (Supplemental Table S5), whereas this was not the case for down-regulated genes (Supplemental Table S6). Differences in the expression of genes with functions related to lactate metabolism and sterol/terpenoid metabolism were particularly noticeable and are discussed in the following sections.

Lactate production decreased in XX/Sry Sertoli cells

It has been established that lactate supplied by Sertoli cells is utilized as an energy source by developing germ cells such as spermatocytes, spermatids, and

spermatozoa[13]. Interestingly, genes related to 'lactate dehydrogenase activity' were among those down-regulated in P21 XX/*Sry* Sertoli cells. Lactate dehydrogenase (LDH) is a tetrameric enzyme of lactate dehydrogenase A (LDHA) and B (LDHB) subunits encoded by *Ldha* and *Ldhb*, respectively. Sequencing indicated that expression of *Ldha* was decreased in P21 XX/*Sry* Sertoli cells, while that of *Ldhb* was slightly increased (Fig. 3a). qRT-PCR analysis confirmed the sequence data (Fig. 3b). As expected, LDHA protein was decreased in P21 XX/*Sry* Sertoli cells (Fig. 3c).

LDH with four subunits of LDHA is known to preferentially mediate conversion from pyruvate to lactate. By contrast, LDH with four subunits of LDHB mediates conversion from lactate to pyruvate[46,47]. In addition to these, three distinct isoenzymes (one A/three B, two A/two B, and three A/one B) can be formed with LDHA and LDHB, and are thought to exhibit an intermediate level of activity[48]. Considering the decreased expression of *Ldha* and increased expression of *Ldhb* in the XX/*Sry* Sertoli cells, lactate production may be lower in these cells.

In addition to synthesis, the lactate transport activity of Sertoli cells should be considered. Monocarboxylate transporters encoded by *Mct1* (*Slc16a1*), *Mct2* (*Slc16a7*), *Mct3* (*Slc16a8*), and *Mct4* (*Slc16a3*) have been identified as lactate transporters. *Mct1* and *Mct4* were found to be expressed in the Sertoli cells, whereas *Mct2* and *Mct3* were mostly absent (Fig. 3a). Sequencing and qRT-PCR analysis indicated that expression of *Mct1* and *Mct4* was decreased slightly and strongly, respectively, in XX/*Sry* Sertoli cells (Fig. 3a, b).

MCT1 and MCT4 are responsible for the import and export of lactate, respectively[49-51]. Considering the down-regulated expression of both *Mct4* and lactate-synthesizing *Ldha*, the quantity of lactate efflux from XX/*Sry* Sertoli cells was expected to be lower. To investigate this, Sertoli cells from XY and XX/*Sry* testes at

P21 were cultured and the quantities of lactate in the culture media determined. Lactate in the media of both types of Sertoli cells was found to increase over time (Fig. 3d). As expected, amounts were significantly higher in XY than in XX/*Sry* Sertoli cells, possibly indicating that the activity of lactate supply to germ cells is strongly impacted in XX/*Sry* Sertoli cells.

Cholesterol production decreased in XX/Sry Sertoli cells

Sertoli cells supply cholesterol to germ cells. The metabolism, influx, and efflux of cholesterol in or from Sertoli cells are therefore critical for germ cell development. Biological functions related to cholesterol and sterol metabolism were found to be associated with genes that were down-regulated in P21 XX/*Sry* Sertoli cells. In fact, sequence data indicated that the expression of many cholesterogenic genes was down-regulated (Fig. 4a). Similarly, qRT-PCR analysis showed that the expression of 13 out of 20 cholesterogenic genes was significantly decreased in XX/*Sry* Sertoli cells (Fig. 4b). Consistent with the results above, immunoblot studies revealed the amount of CYP51 protein decreased in XX/*Sry* Sertoli cells. Unexpectedly, however, the amount of HMGCR was unchanged (Fig. 4c). Since the amount of HMGCR is regulated post-translationally[52], HMGCR might be stabilized in XX/*Sry* Sertoli cells.

SREBP2 (sterol regulatory element binding protein 2), also known as SREBF2, has been established as the master regulator of cholesterogenic gene transcription[53,54]. My results obtained by sequencing (Fig. 5a) and qRT-PCR analysis (Fig. 5b) showed a significantly decreased expression of *Srebf2* but unaffected expressions of *Sox9, Ad4BP/SF-1, Dmrt1, Amh,* and *Dhh* in XX/*Sry* Sertoli cells. I consequently investigated whether the decreased expression of *Srebf2* led to a decrease in cholesterogenic gene expression in XY Sertoli cells. siRNA treatment successfully

decreased the expression of *Srebf2* (Fig. 5c). qRT-PCR of cholesterogenic genes revealed that eight genes were suppressed by the treatment (Fig. 5d). Seven of these (*Hmgcr*, *Idi1*, *Sqle*, *Cyp51*, *Msmo1*, *Hsd17b7*, and *Dhcr24*) were among the genes down-regulated in XX/*Sry* Sertoli cells, suggesting that the down-regulation of the cholesterogenic genes was primarily the result of the decreased expression of *Srebf2*.

Influx and efflux as well as synthesis should be considered in cholesterol homeostasis. Influx of cholesterol into Sertoli cells is predominantly mediated by HDL receptor/SRB1 encoded by *Scarb1*, while efflux is mediated by ABCA1 encoded by *Abca1*[16,55]. Sequencing and qRT-PCR analysis indicated that the expression of *Scarb1* was not affected and that *Abca1* expression was unlikely to be down-regulated in XX/*Sry* Sertoli cells (Fig. 5a, b).

Since these results strongly suggested that cholesterol synthesis is affected in XX/*Sry* Sertoli cells, I investigated cholesterogenic activity. The amount of ^{14}C-labeled free cholesterol in cultured XX/*Sry* Sertoli cells was 60% of that in XY Sertoli cells (Fig. 6a). I also determined the quantities of cholesterol together with lanosterol, lathosterol, and desmosterol, all of which are intermediate molecules in the cholesterogenic pathway (Fig. 6b). As expected, the amounts of lathosterol and desmosterol were substantially smaller in XX/*Sry* Sertoli cells (Fig. 6c). Unexpectedly, this was not the case for cholesterol. This may be because the germ cells had mostly disappeared from the XX/*Sry* testes by P21 and the Sertoli cells had thus lost the cells to which they would have transferred their cholesterol.

Differential epigenetic regulation in XY and XX/Sry Sertoli cells

Since *Uty* and *Smcy* are localized on the Y chromosome, transcripts of these genes were undetectable in XX/*Sry* Sertoli cells by either sequencing or qRT-PCR

(Fig. 7a, b). The expression of *Utx* and *Smcx* was roughly consistent with the gene dosage (a single copy in XY and two copies in XX/*Sry* Sertoli cells). This dosage-dependent expression is consistent with the observation that these genes escape from X chromosome inactivation[56,57]. Interestingly, the FPKM value of *Smcx* was 10-fold higher than that of *Smcy*, suggesting that the demethylation activity of H3K4me3 was stronger in XX/*Sry* than in XY Sertoli cells, assuming that its protein products could mediate demethylation with similar enzyme specific activity.

These differential expressions of histone modification enzymes raise the possibility that the methylation status of H3K4 and H3K27 was different in the two types of Sertoli cells. To examine this, I performed genome-wide ChIP-sequencing of both types of Sertoli cells at P21 using the antibodies for H3K4me3 and H3K27me3. H3K4me3 was found to be accumulated around the TSS of genes (Fig. 7c). As expected, the accumulation was substantially lower in XX/*Sry* Sertoli cells, possibly due to higher expression of *Smcx*. The accumulation of H3K27me3 distributed along the gene body was slightly higher in XX/*Sry* than XY Sertoli cells.

I then examined whether the differential status of active H3K4me3 and suppressive H3K27me3 was relevant to the differential gene expression in XY and XX/*Sry* Sertoli cells. As expected, the accumulation of H3K4me3 was greater at the TSS of genes that were up-regulated in XX/*Sry* Sertoli cells ($p < 0.01$), while accumulation was lower around down-regulated genes ($p < 0.001$; Fig. 7d). Accumulation of H3K27me3 was greater around genes that were down-regulated in XX/*Sry* Sertoli cells ($p < 0.01$), while there was no significant accumulation around up-regulated genes ($p = 0.268$).

The expression of *Ldha* and *Mct4*, implicated in the supply of lactate to germ cells, was down-regulated in XX/*Sry* Sertoli cells as described above (Fig. 3b).

Consistent with this finding, the accumulation of active H3K4me3 and suppressive H3K27me3 was smaller and greater, respectively, at both *Ldha* and *Mct4* gene loci (Fig. 7e). As noted above, the expression of 13 genes involved in cholesterogenesis was down-regulated in XX/*Sry* Sertoli cells (Fig. 4b). H3K4me3 was decreased to varying degrees around most cholesterogenic genes except *Acta2*, *Mvd*, and *Fdft1*. An increased tendency for H3K27me3 accumulation was observed in more than half of the cholesterogenic genes.

These histone modifications (decreased H3K4me3 and increased H3K27me3) probably lead to the down-regulation of gene expression. In fact, among the 13 cholesterogenic genes down-regulated in XX/*Sry* Sertoli cells, such changes were observable in *Hmgcr*, *Mvk*, *Fdps*, *Sqle*, *Lss*, *Nsdhl*, *Sc5d*, and *Dhcr24*. As described above, I examined which genes were affected by the down-regulation of *Srebf2* in XX/*Sry* Sertoli cells, and to my surprise found that the expression of *Mvk*, *Mvd*, *Fdps*, *Lss*, *Nsdhl*, and *Scd5d* was not subject to down-regulation as a result of *Srebf2* knockdown. The chromatin state of all these gene loci (with the exception of *Mvd*) was changed from active to inactive as a result of the decrease in H3K4me3 and increase in H3K27me3. These epigenetic changes might induce the down-regulation of gene expression independently of SREBF2 function in XX/*Sry* Sertoli cells. It should also be noted that the accumulation of H3K4me3 was lower in *Srebf2*, possibly causing the down-regulation of cholesterogenic genes.

DISCUSSION

To achieve a better understanding of the functional differences between XY and XX/*Sry* Sertoli cells, I compared the mRNA expression profiles of the two cell types and determined which gene expressions were up- or down-regulated in XX/*Sry* Sertoli cells. GO and KEGG pathway analyses suggested that lactate and cholesterol metabolisms are impaired in XX/*Sry* Sertoli cells. Considering that the function of Sertoli cells is the nursing of developing germ cells, these effects on metabolic pathways are intriguing.

The energy metabolic pathway functioning in male germ cells is known to change during the course of differentiation from spermatogonia to spermatozoa[11]. Spermatogonia use glucose as fuel for ATP production, spermatocytes begin to utilize lactate, and later-stage germ cells such as spermatids and spermatozoa are highly depend on lactate as an energy source[12,13]. The carbohydrate metabolism of Sertoli cells is unusual; only 25% of the pyruvate produced by glycolysis is oxidized by the TCA cycle[58], and cultured Sertoli cells mediate reactions from glucose to lactate via pyruvate[59]. This lactate is thought to be supplied to the developing germ cells.

The present study demonstrates that the expression of genes related to lactate metabolism differs between XY and XX/*Sry* Sertoli cells. Quantitative studies have found that *Ldha* is down-regulated in XX/*Sry* Sertoli cells, suggesting the possibility that lactate supply to developing germ cells is reduced in XX/*Sry* testes. This might be supported by the transplantation study of XY germ cells into XX/*Sry* testes performed by Ishii *et al*[6]. Although the transplanted XY germ cells were capable of completing meiosis, their differentiation into elongated spermatids was impaired in the milieu established by the XX/*Sry* Sertoli cells. Considering that the predominant energy fuel shifts from glucose to lactate at the spermatocyte or spermatozoon stage, it can be

assumed that a lower supply of lactate impedes the differentiation of the spermatocyte into an elongated spermatid.

Another crucial nursing function of Sertoli cells is thought to be the supply of cholesterol to germ cells[14]. Cholesterol homeostasis in Sertoli cells is preserved in several ways, such as *de novo* synthesis, influx via the HDL receptor, and efflux via the ABCA1 transporter. Perturbation of cholesterol homeostasis by disruption of *Abca1* resulted in significantly affected spermatogenesis and fertility, in addition to abnormal lipid accumulation in the Sertoli cells[18].

My study demonstrated that expression of 13 of the 20 cholesterogenic genes was significantly down-regulated in XX/*Sry* Sertoli cells. Probably because of this suppressed gene expression, *de novo* cholesterol synthetic activity was lower in XX/*Sry* than in XY Sertoli cells. Expression of *Abca1* and *Scarb1* (involved in influx and efflux of cholesterol) was not markedly affected, suggesting that cholesterol transfer remains normal in XX/*Sry* Sertoli cells and that they consequently should feature lower quantities of intracellular cholesterol. However, no difference in the amount of free and esterified cholesterol in the two Sertoli cell types was found. While I are unable to suggest a plausible explanation for this apparent contradiction, the disappearance of germ cells from XX/*Sry* testes might affect the functioning of the XX/*Sry* Sertoli cells by removing the targets of their cholesterol transfer, thus preventing a decrease in their cholesterol content.

Determining the causes of the differential expression of metabolic genes in XX/*Sry* Sertoli cells is an important aim of this research. The cholesterogenic gene *Srebf2,* encoding an already-known key factor for cholesterogenic gene regulation[53,54], was found to be down-regulated in XX/*Sry* Sertoli cells, suggesting a knockdown experiment to determine whether down-regulated *Srebf2* results in reduced expression

of cholesterogenic genes. This experiment confirmed the decreased expression of seven of the 13 genes whose expression was down-regulated in XX/*Sry* Sertoli cells. It was therefore assumed that the remaining six genes were regulated by a mechanism independent of SREBF2.

A candidate for the regulation mechanism was suggested by the fact that the genes encoding histone modification enzymes are localized on the sex chromosomes. SMCX on the X and SMCY on the Y chromosome mediate the demethylation of an active histone mark, H3K4me3[21]. UTX mediates the demethylation of a suppressive histone mark, H3K27me3, whereas UTY does not exhibit this activity[22,23]. Because of the differential expression of these genes in XY and XX/*Sry* Sertoli cells, it was assumed that the methylation statuses of H3K4 and H3K27 were affected accordingly. Importantly, these epigenetic changes occurred in many, if not all, of the cholesterogenic genes, and I therefore suspect that they cause the down-regulation of cholesterogenic gene expression in XX/*Sry* Sertoli cells.

These observations may support the idea that *Smcx*/*Smcy* and *Utx*/*Uty*, which are localized on the sex chromosomes, regulate sexually dimorphic gene expression. Indeed, an *Utx* gene knockout study demonstrated that UTX regulates the level of H3K27me3, suggesting that the difference in *Utx* gene dosage between the two sexes leads to sex-dependent deposition of H3K27me3[29]. Sex-dependent differences in deposition of H3K27me3 were also identified in hepatocytes and primordial germ cells[60,61].

Gene expression in Sertoli cells is regulated by the testosterone and androgen receptor, AR (NR3C4)[62]. Upon ligand binding, AR forms protein complexes with histone modification enzymes, thereby changing chromatin structure to regulate target gene expression[63,64]. Plasma testosterone in XX/*Sry* mice was found to be lower than

that in XY males. Although testosterone did not completely disappear from XX/*Sry* mice, this decrease may lead to a suppression of AR target gene expression. Because it is unclear whether the genes involved in lactate and cholesterol metabolism are targets of AR, I cannot exclude the possibility that the decreased expression of those genes is due to the decreased testosterone. Identification of AR target genes in Sertoli cells would be needed to resolve this issue.

In summary, I examined the functional differences between XY and XX/*Sry* Sertoli cells and demonstrated that lactate and cholesterol metabolism, both of which play a crucial role in the nursing of developing germ cells, are down-regulated in XX/*Sry* Sertoli cells. Moreover, my results suggest that these differential functions are at least in part the result of differential expression of histone modification enzymes encoded by sex chromosomes. Although it is well known that XX testes cannot support the differentiation of germ cells even if they carry XY chromosomes, the reason for this has remained unclear. This study suggests that this phenomenon may be caused by the down-regulation of lactate and cholesterol metabolism resulting from altered epigenetic modification.

REFERENCE

1 Koopman, P., Munsterberg, A., Capel, B., Vivian, N. & Lovell-Badge, R. Expression of a candidate sex-determining gene during mouse testis differentiation. *Nature* **348**, 450-452, doi:10.1038/348450a0 (1990).

2 Kashimada, K. & Koopman, P. Sry: the master switch in mammalian sex determination. *Development* **137**, 3921-3930, doi:10.1242/dev.048983 (2010).

3 Larney, C., Bailey, T. L. & Koopman, P. Switching on sex: transcriptional regulation of the testis-determining gene Sry. *Development* **141**, 2195-2205, doi:10.1242/dev.107052 (2014).

4 Ross, A. J. & Capel, B. Signaling at the crossroads of gonad development. *Trends Endocrinol Metab* **16**, 19-25, doi:10.1016/j.tem.2004.11.004 (2005).

5 Koopman, P., Gubbay, J., Vivian, N., Goodfellow, P. & Lovell-Badge, R. Male development of chromosomally female mice transgenic for Sry. *Nature* **351**, 117-121, doi:10.1038/351117a0 (1991).

6 Ishii, M. *et al.* Potency of testicular somatic environment to support spermatogenesis in XX/Sry transgenic male mice. *Development* **134**, 449-454, doi:10.1242/dev.02751 (2007).

7 Cattanach, B. M. Sex-reversed mice and sex determination. *Ann N Y Acad Sci* **513**, 27-39 (1987).

8 Burgoyne, P. S. The role of the mammalian Y chromosome in spermatogenesis. *Development* **101 Suppl**, 133-141 (1987).

9 Cheng, C. Y., Wong, E. W., Yan, H. H. & Mruk, D. D. Regulation of spermatogenesis in the microenvironment of the seminiferous epithelium: new insights and advances. *Mol Cell Endocrinol* **315**, 49-56, doi:10.1016/j.mce.2009.08.004 (2010).

10 Wenger, R. H. & Katschinski, D. M. The hypoxic testis and post-meiotic expression of PAS domain proteins. *Seminars in cell & developmental biology* **16**, 547-553, doi:10.1016/j.semcdb.2005.03.008 (2005).

11 Bajpai, M., Gupta, G. & Setty, B. S. Changes in carbohydrate metabolism of testicular germ cells during meiosis in the rat. *Eur J Endocrinol* **138**, 322-327 (1998).

12 Boussouar, F. & Benahmed, M. Lactate and energy metabolism in male germ cells. *Trends Endocrinol Metab* **15**, 345-350, doi:10.1016/j.tem.2004.07.003 (2004).

13 Rato, L. *et al.* Metabolic regulation is important for spermatogenesis. *Nat Rev Urol* **9**, 330-338, doi:10.1038/nrurol.2012.77 (2012).

14 Keber, R., Rozman, D. & Horvat, S. Sterols in spermatogenesis and sperm maturation. *J Lipid Res* **54**, 20-33, doi:10.1194/jlr.R032326 (2013).

15 Wiebe, J. P. & Tilbe, K. S. De novo synthesis of steroids (from acetate) by isolated rat Sertoli cells. *Biochem Biophys Res Commun* **89**, 1107-1113 (1979).

16 Fofana, M., Travert, C., Carreau, S. & Le Goff, D. Evaluation of cholesteryl ester transfer in the seminiferous tubule cells of immature rats in vivo and in vitro. *J Reprod Fertil* **118**, 79-83 (2000).

17 Gillot, I. *et al.* Germ cells and fatty acids induce translocation of CD36 scavenger receptor to the plasma membrane of Sertoli cells. *J Cell Sci* **118**, 3027-3035, doi:10.1242/jcs.02430 (2005).

18 Selva, D. M. *et al.* The ATP-binding cassette transporter 1 mediates lipid efflux from Sertoli cells and influences male fertility. *J Lipid Res* **45**, 1040-1050, doi:10.1194/jlr.M400007-JLR200 (2004).

19 Vernet, N. *et al.* Retinoid X receptor beta (RXRB) expression in Sertoli cells controls cholesterol homeostasis and spermiation. *Reproduction* **136**, 619-626, doi:10.1530/rep-08-0235 (2008).

20 Volle, D. H. *et al.* Multiple roles of the nuclear receptors for oxysterols liver X receptor to maintain male fertility. *Molecular endocrinology* **21**, 1014-1027, doi:10.1210/me.2006-0277 (2007).

21 Iwase, S. *et al.* The X-linked mental retardation gene SMCX/JARID1C defines a family of histone H3 lysine 4 demethylases. *Cell* **128**, 1077-1088, doi:10.1016/j.cell.2007.02.017 (2007).

22 Hong, S. *et al.* Identification of JmjC domain-containing UTX and JMJD3 as histone H3 lysine 27 demethylases. *Proc Natl Acad Sci U S A* **104**, 18439-18444, doi:10.1073/pnas.0707292104 (2007).

23 Lan, F. *et al.* A histone H3 lysine 27 demethylase regulates animal posterior development. *Nature* **449**, 689-694, doi:10.1038/nature06192 (2007).

24 Santos-Rosa, H. *et al.* Active genes are tri-methylated at K4 of histone H3. *Nature* **419**, 407-411, doi:10.1038/nature01080 (2002).

25 Kirmizis, A. *et al.* Silencing of human polycomb target genes is associated with methylation of histone H3 Lys 27. *Genes Dev* **18**, 1592-1605, doi:10.1101/gad.1200204 (2004).

26 Justin, N., De Marco, V., Aasland, R. & Gamblin, S. J. Reading, writing and editing methylated lysines on histone tails: new insights from recent structural studies. *Curr Opin Struct Biol* **20**, 730-738, doi:10.1016/j.sbi.2010.09.012 (2010).

27 Lee, S., Lee, J. W. & Lee, S. K. UTX, a histone H3-lysine 27 demethylase, acts as a critical switch to activate the cardiac developmental program. *Dev Cell* **22**, 25-37, doi:10.1016/j.devcel.2011.11.009 (2012).

28 Wang, C. *et al.* UTX regulates mesoderm differentiation of embryonic stem cells independent of H3K27 demethylase activity. *Proc Natl Acad Sci U S A* **109**, 15324-15329, doi:10.1073/pnas.1204166109 (2012).

29 Welstead, G. G. *et al.* X-linked H3K27me3 demethylase Utx is required for embryonic development in a sex-specific manner. *Proc Natl Acad Sci U S A* **109**, 13004-13009, doi:10.1073/pnas.1210787109 (2012).

30 Kidokoro, T. *et al.* Influence on spatiotemporal patterns of a male-specific Sox9 activation by ectopic Sry expression during early phases of testis differentiation in mice. *Dev Biol* **278**, 511-525, doi:10.1016/j.ydbio.2004.11.006 (2005).

31 Nakamura, Y. *et al.* Wwp2 is essential for palatogenesis mediated by the interaction between Sox9 and mediator subunit 25. *Nat Commun* **2**, 251, doi:10.1038/ncomms1242 (2011).

32 Shima, Y. *et al.* Contribution of Leydig and Sertoli cells to testosterone production in mouse fetal testes. *Molecular endocrinology* **27**, 63-73, doi:10.1210/me.2012-1256 (2013).

33 Shima, Y. *et al.* Identification of an enhancer in the Ad4BP/SF-1 gene specific for fetal Leydig cells. *Endocrinology* **153**, 417-425, doi:10.1210/en.2011-1407 (2012).

34 Baba, T. *et al.* Glycolytic genes are targets of the nuclear receptor Ad4BP/SF-1. *Nat Commun* **5**, 3634, doi:10.1038/ncomms4634 (2014).

35 Trapnell, C., Pachter, L. & Salzberg, S. L. TopHat: discovering splice junctions with RNA-Seq. *Bioinformatics* **25**, 1105-1111, doi:10.1093/bioinformatics/btp120 (2009).

36 Li, B. & Dewey, C. N. RSEM: accurate transcript quantification from RNA-Seq data with or without a reference genome. *BMC Bioinformatics* **12**, 323, doi:10.1186/1471-2105-12-323 (2011).

37 Trapnell, C. *et al.* Transcript assembly and quantification by RNA-Seq reveals unannotated transcripts and isoform switching during cell differentiation. *Nat Biotechnol* **28**, 511-515, doi:10.1038/nbt.1621 (2010).

38 Ashburner, M. *et al.* Gene ontology: tool for the unification of biology. The Gene Ontology Consortium. *Nat Genet* **25**, 25-29, doi:10.1038/75556 (2000).

39 Huang da, W. *et al.* Extracting biological meaning from large gene lists with DAVID. *Curr Protoc Bioinformatics* **Chapter 13**, Unit 13.11, doi:10.1002/0471250953.bi1311s27 (2009).

40 Lorbek, G. *et al.* Lessons from hepatocyte-specific Cyp51 knockout mice: impaired cholesterol synthesis leads to oval cell-driven liver injury. *Scientific reports* **5**, 8777, doi:10.1038/srep08777 (2015).

41 Langmead, B., Trapnell, C., Pop, M. & Salzberg, S. L. Ultrafast and memory-efficient alignment of short DNA sequences to the human genome. *Genome Biol* **10**, R25, doi:10.1186/gb-2009-10-3-r25 (2009).

42 Quinlan, A. R. & Hall, I. M. BEDTools: a flexible suite of utilities for comparing genomic features. *Bioinformatics* **26**, 841-842, doi:10.1093/bioinformatics/btq033 (2010).

43 Gafni, O. *et al.* Derivation of novel human ground state naive pluripotent stem cells. *Nature* **504**, 282-286, doi:10.1038/nature12745 (2013).

44 Son, H. H. *et al.* High-temperature GC-MS-based serum cholesterol signatures may reveal sex differences in vasospastic angina. *J Lipid Res* **55**, 155-162, doi:10.1194/jlr.D040790 (2014).

45 Star-Weinstock, M., Williamson, B. L., Dey, S., Pillai, S. & Purkayastha, S. LC-ESI-MS/MS analysis of testosterone at sub-picogram levels using a novel derivatization reagent. *Analytical chemistry* **84**, 9310-9317, doi:10.1021/ac302036r (2012).

46 Cahn, R. D., Zwilling, E., Kaplan, N. O. & Levine, L. Nature and Development of Lactic Dehydrogenases: The two major types of this enzyme form molecular hybrids which change in makeup during development. *Science* **136**, 962-969, doi:10.1126/science.136.3520.962 (1962).

47 Dawson, D. M., Goodfriend, T. L. & Kaplan, N. O. LACTIC DEHYDROGENASES: FUNCTIONS OF THE TWO TYPES RATES OF SYNTHESIS OF THE TWO MAJOR FORMS CAN BE CORRELATED WITH METABOLIC DIFFERENTIATION. *Science* **143**, 929-933 (1964).

48 Krieg, A. F., Rosenblum, L. J. & Henry, J. B. Lactate dehydrogenase isoenzymes a comparison of pyruvate-to-lactate and lactate-to-pyruvate assays. *Clin Chem* **13**, 196-203 (1967).

49 McCullagh, K. J., Poole, R. C., Halestrap, A. P., O'Brien, M. & Bonen, A. Role of the lactate transporter (MCT1) in skeletal muscles. *Am J Physiol* **271**, E143-150 (1996).

50 Dimmer, K. S., Friedrich, B., Lang, F., Deitmer, J. W. & Broer, S. The low-affinity monocarboxylate transporter MCT4 is adapted to the export of lactate in highly glycolytic cells. *Biochem J* **350 Pt 1**, 219-227 (2000).

51 Galardo, M. N., Riera, M. F., Pellizzari, E. H., Cigorraga, S. B. & Meroni, S. B. The AMP-activated protein kinase activator, 5-aminoimidazole-4-carboxamide-1-b-D-ribonucleoside, regulates lactate production in rat Sertoli cells. *J Mol Endocrinol* **39**, 279-288, doi:10.1677/jme-07-0054 (2007).

52 Goldstein, J. L., DeBose-Boyd, R. A. & Brown, M. S. Protein sensors for membrane sterols. *Cell* **124**, 35-46, doi:10.1016/j.cell.2005.12.022 (2006).

53 Pai, J. T., Guryev, O., Brown, M. S. & Goldstein, J. L. Differential stimulation of cholesterol and unsaturated fatty acid biosynthesis in cells expressing individual nuclear sterol regulatory element-binding proteins. *J Biol Chem* **273**, 26138-26148 (1998).

54 Horton, J. D. *et al.* Activation of cholesterol synthesis in preference to fatty acid synthesis in liver and adipose tissue of transgenic mice overproducing sterol regulatory element-binding protein-2. *J Clin Invest* **101**, 2331-2339, doi:10.1172/jci2961 (1998).

55 Akpovi, C. D., Yoon, S. R., Vitale, M. L. & Pelletier, R. M. The predominance of one of the SR-BI isoforms is associated with increased esterified cholesterol levels not apoptosis in mink testis. *J Lipid Res* **47**, 2233-2247, doi:10.1194/jlr.M600162-JLR200 (2006).

56 Agulnik, A. I. *et al.* A novel X gene with a widely transcribed Y-linked homologue escapes X-inactivation in mouse and human. *Hum Mol Genet* **3**, 879-884 (1994).

57 Greenfield, A. *et al.* The UTX gene escapes X inactivation in mice and humans. *Hum Mol Genet* **7**, 737-742 (1998).

58 Grootegoed, J. A., Oonk, R. B., Jansen, R. & van der Molen, H. J. Metabolism of radiolabelled energy-yielding substrates by rat Sertoli cells. *J Reprod Fertil* **77**, 109-118 (1986).

59 Robinson, R. & Fritz, I. B. Metabolism of glucose by Sertoli cells in culture. *Biol Reprod* **24**, 1032-1041 (1981).

60 Sugathan, A. & Waxman, D. J. Genome-wide analysis of chromatin states reveals distinct mechanisms of sex-dependent gene regulation in male and female mouse liver. *Mol Cell Biol* **33**, 3594-3610, doi:10.1128/mcb.00280-13 (2013).

61 Brind'Amour, J. *et al.* An ultra-low-input native ChIP-seq protocol for genome-wide profiling of rare cell populations. *Nat Commun* **6**, 6033, doi:10.1038/ncomms7033 (2015).

62 Smith, L. B. & Walker, W. H. The regulation of spermatogenesis by androgens. *Seminars in cell & developmental biology* **30**, 2-13, doi:10.1016/j.semcdb.2014.02.012 (2014).

63 Leader, J. E., Wang, C., Fu, M. & Pestell, R. G. Epigenetic regulation of nuclear steroid receptors. *Biochemical pharmacology* **72**, 1589-1596, doi:10.1016/j.bcp.2006.05.024 (2006).

64 Kim, J. Y., Yu, J., Abdulkadir, S. A. & Chakravarti, D. KAT8 Regulates Androgen Signaling in Prostate Cancer Cells. *Molecular endocrinology* **30**, 925-936, doi:10.1210/me.2016-1024 (2016).

ACKNOWLEDGEMENTS

First and foremost I would like to express my sincere gratitude to my advisor Prof. Ken-ichirou Morohashi for the continuous support of my PhD study and related research, for his patience, motivation, and immense knowledge. I appreciate all his contributions of time, ideas, and funding to make my PhD. experience productive and stimulating. I could not have imagined having a better advisor and mentor for my PhD study.

Many thanks also to Dr. Takeshi Baba who taught me how to ask questions and express my ideas. In addition to his fine technical instruction, he showed me different ways to approach a research problem and the need to be persistent to accomplish any goal.

Besides, Dr. Tetsuya Sato and Dr. Mikita Suyama (Division of Bioinformatics, Medical Institute of Bioregulation, Kyushu University) are thanked for technical discussion and contribution to the computational analyses for mRNA-seq and ChIP-seq. I thank Dr. Haruhiko Akiyama (Department of Orthopaedics, Gifu University Graduate School of Medicine) and Dr. Yoshiakira Kanai (Department of Veterinary Anatomy, The University of Tokyo) for their kindly gift of mice. I appreciate Dr. Kimura Hiroshi (Department of Biological Sciences, Graduate School of Bioscience and Biotechnology, Tokyo Institute of Technology) and Dr. Damjana Rozman (Centre for Functional Genomics and Bio-Chips, Institute of Biochemistry, Faculty of Medicine, University of Ljubljana) gifting me their valuable antibodies. In regards to the measurement of cholesterol metabolites, I thank Dr. Yasuhiro Ishihara (Graduate School of Integrated Arts and Sciences, Hiroshima University) and Dr. Man-Ho Choi (Molecular Recognition Research Center, Korea Institute of Science and Technology) for significant contributions to the experiments. I am grateful to Dr. Shogo Haraguchi

and Dr. Akira Miyazaki (Department of Biochemistry, Showa University School of Medicine) for their efforts in determining testosterone concentration. I also appreciate Dr. Yasuyuki Ohkawa (Research Center for Transomics Medicine, Medical Institute of Bioregulation, Kyushu University) for deep sequencing of the mRNA-seq and ChIP-seq libraries. Special thanks should also be given to Miki Inoue. I couldn't finish my project without her support in performing experiences and preparing manuscripts for my prepublication paper.

I would like to appreciate Dr. Yuichi Shima, Dr. Kanako Shima-Miyabayashi and Dr. Hiroyuki Otake for their technical supports and practical advice. I thank my fellow labmates in Morohashi's laboratory, Li Bing, Miki Inoue and Sawako Matsuzaki, for the stimulating discussions, for the busy and nervous days we were working together before deadlines, and for all the fun we shared.

Last but not the least, I would like to express my deepest gratitude to my family. This dissertation would not have been possible without their warm love, continued patience, and endless support.

FIGURES

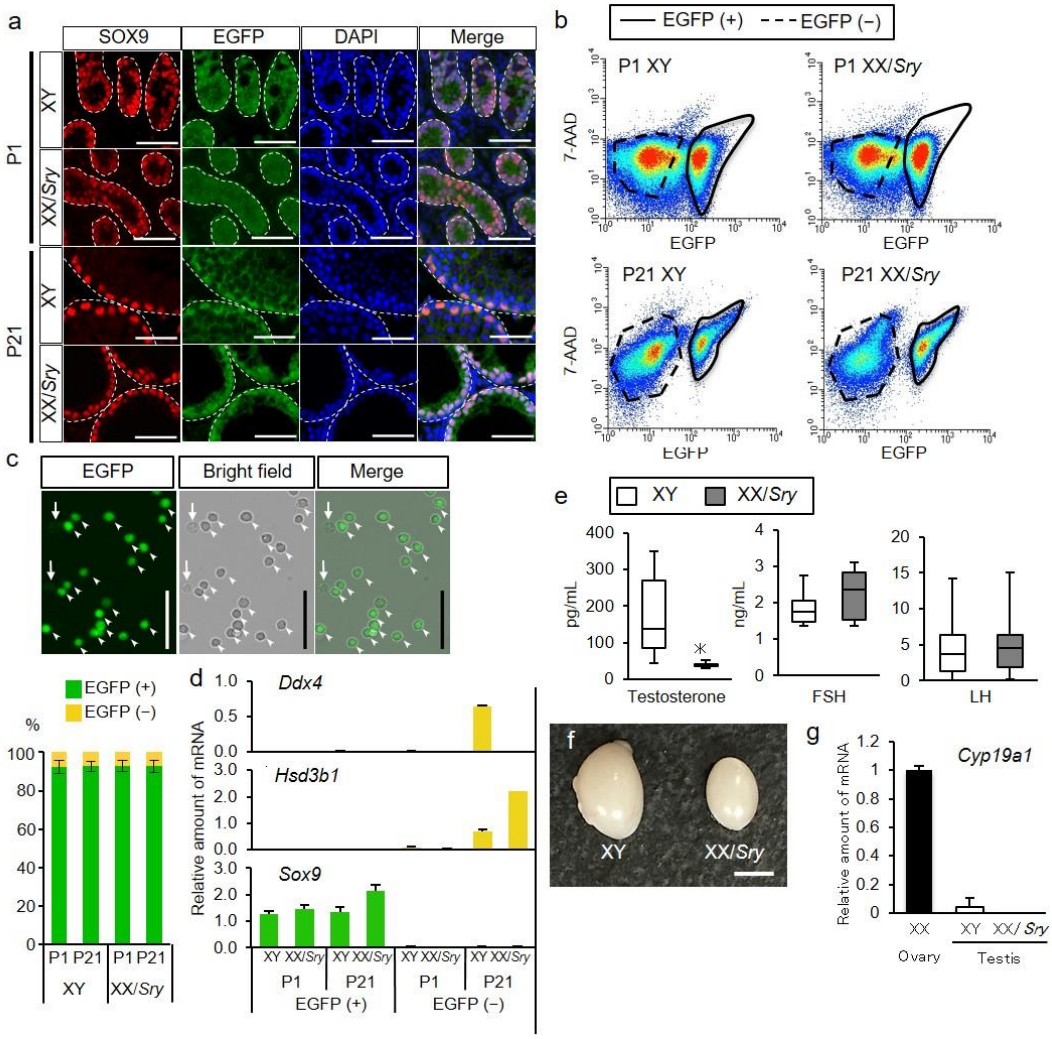

Fig. 1, Preparation of XY and XX/Sry Sertoli cells

a, Testes from XY and XX/*Sry* mice at P1 and P21 were immunostained with antibodies for SOX9 (red) and EGFP (green). Nuclei were stained with DAPI (blue). Merged images are shown in the right-hand panel. Seminiferous tubules are surrounded by white broken lines. Scale bars = 50 μm. **b**, Testicular cells from XY and XX/*Sry* mice at P1 and P21 were fractioned by FACS. Fractions surrounded by solid lines were recovered as EGFP-positive cells, while fractions surrounded by broken lines were recovered as EGFP-negative cells. **c**, Fluorescence and bright field images of the EGFP-positive cells from the P21 XY testes. The EGFP-positive (arrowheads) and EGFP-negative cells (arrows) were counted, and ratios of EGFP-positive (green) to EGFP-negative cells (yellow) are shown. **d**, RNAs prepared from the EGFP-positive (green bars) and EGFP-negative (yellow bars) cells were used for qRT-PCR of *Ddx4* (germ cell marker), *Hsd3b1* (Leydig cell marker), and *Sox9*

(Sertoli cell marker). The quantity of mRNA relative to *Actb* (encoding beta-actin) is indicated. **e**, Concentration of testosterone, FSH, and LH were determined in XY and XX/*Sry* mice at P21. The blood samples for XY (n=6) and XX/*Sry* mice (n=6) were used for testosterone assays, while those for XY (n=7) and XX/*Sry* mice (n=6) were used for FSH and LH assays. *$p<0.05$. **f**, Whole view of XY and XX/*Sry* testes are shown. Scale bar=2 mm. **g**, The expression of *Cyp19* in XX ovary, and XY and XX/*Sry* testes was examined by qRT-PCR. The quantity of mRNA relative to *Actb* is indicated. Three biologically independent samples (n=3) were used for the qRT-PCR studies in **d** and **g**.

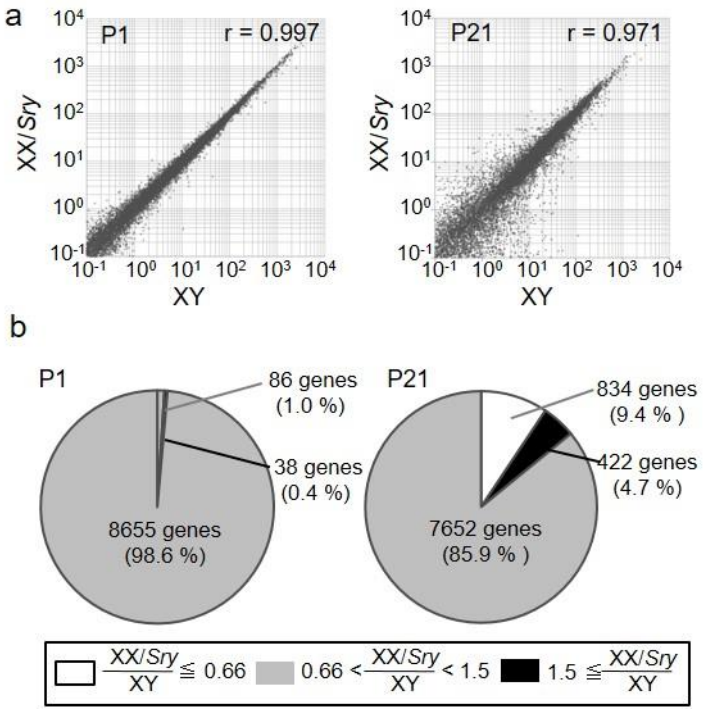

Fig. 2, Gene expression in XY and XX/Sry Sertoli cells

a, Comparison of gene expression levels (FPKM) in XY and XX/*Sry* Sertoli cells at P1 and P21. FPKM values of gene expression in XY Sertoli cells (*x*-axis) and XX/*Sry* (*y*-axis) cells are presented on a log scale; r: relative correlation. **b,** Proportion of genes up- or down-regulated in XX/*Sry* Sertoli cells relative to XY Sertoli cells at P1 and P21.

a

Gene symbol	FPKM XY	FPKM XX/*Sry*	Fold change
Ldha	74.06	46.07	0.62
Ldhb	1133.02	1354.71	1.20
Mct1 (Slc16a1)	64.16	54.34	0.85
Mct2 (Slc16a7)	1.64	1.58	0.96
Mct3 (Slc16a8)	0.32	0.13	0.41
Mct4 (Slc16a3)	48.91	10.47	0.21

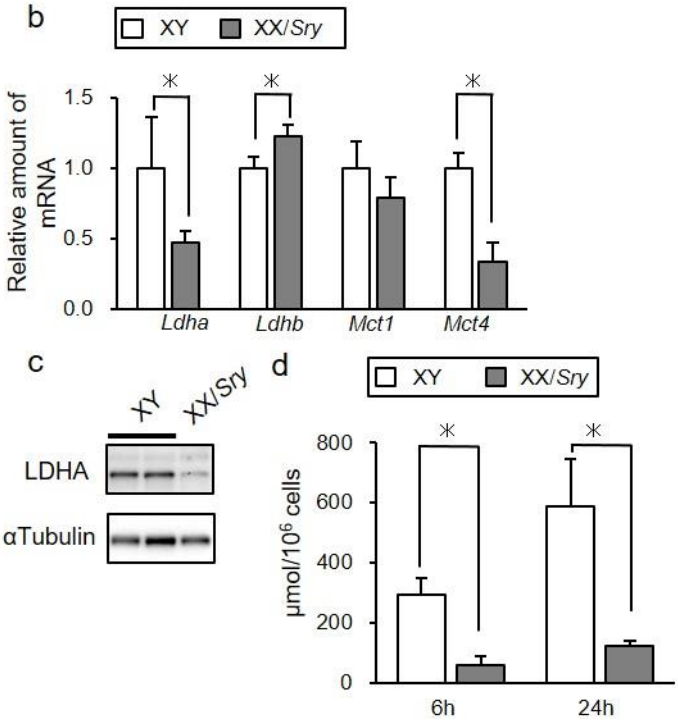

Fig. 3, Lactate production decreased in XX/Sry Sertoli cells

a, Expression levels of lactate dehydrogenase subunits (*Ldha* and *Ldhb*) and monocarboxylate transporters (*Mct1 (Slc16a1), Mct2 (Slc16a7), Mct3 (Slc16a8),* and *Mct4 (Slc16a3)*) in XY and XX/*Sry* Sertoli cells at P21. **b**, Expression of *Ldha*, *Ldhb*, *Mct1*, and *Mct4* in XY and XX/*Sry* Sertoli cells was validated by qRT-PCR analysis. The average values for XY Sertoli cells were normalized to 1.0. **c**, Total cell lysates were prepared from XY and XX/*Sry* testes and then subjected to immunoblot analyses with antibodies for LDHA (upper) and α–tubuline (lower). **d**, XY and XX/*Sry* Sertoli cells (5×10^5) prepared from P21 testes were cultured. Quantities of lactate in the culture media were determined at 6 and 24 h after medium change. The study was performed three times with biologically independent Sertoli cell samples. Three biologically independent samples (n=3) were used for the qRT-PCR studies in **b** and **d**. $*p < 0.05$.

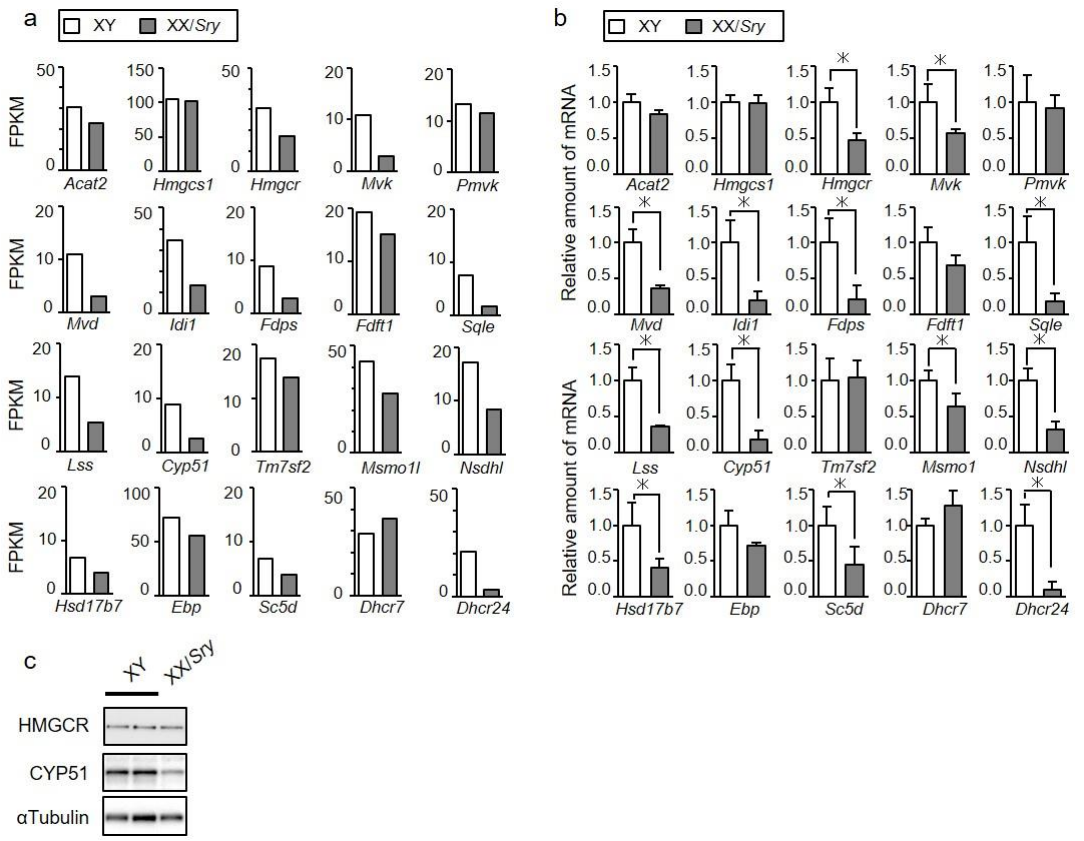

Fig. 4, Decreased expression of cholesterogenic genes in XX/Sry Sertoli cells

a, FPKM values of cholesterogenic genes obtained from mRNA sequencing. **b,** Cholesterogenic gene expression was examined by qRT-PCR with RNAs prepared from XY and XX/*Sry* Sertoli cells. The average values for the XY Sertoli cells were normalized to 1.0. **c,** The amounts of HMGCR and CYP51 in XY and XX/*Sry* Sertoli cells were examined with immunoblotting. α–Tubulin was used as the control. Average values and SDs are indicated. Three biologically independent samples (n=3) were used for the qRT-PCR study in **b.** *$p < 0.05$.

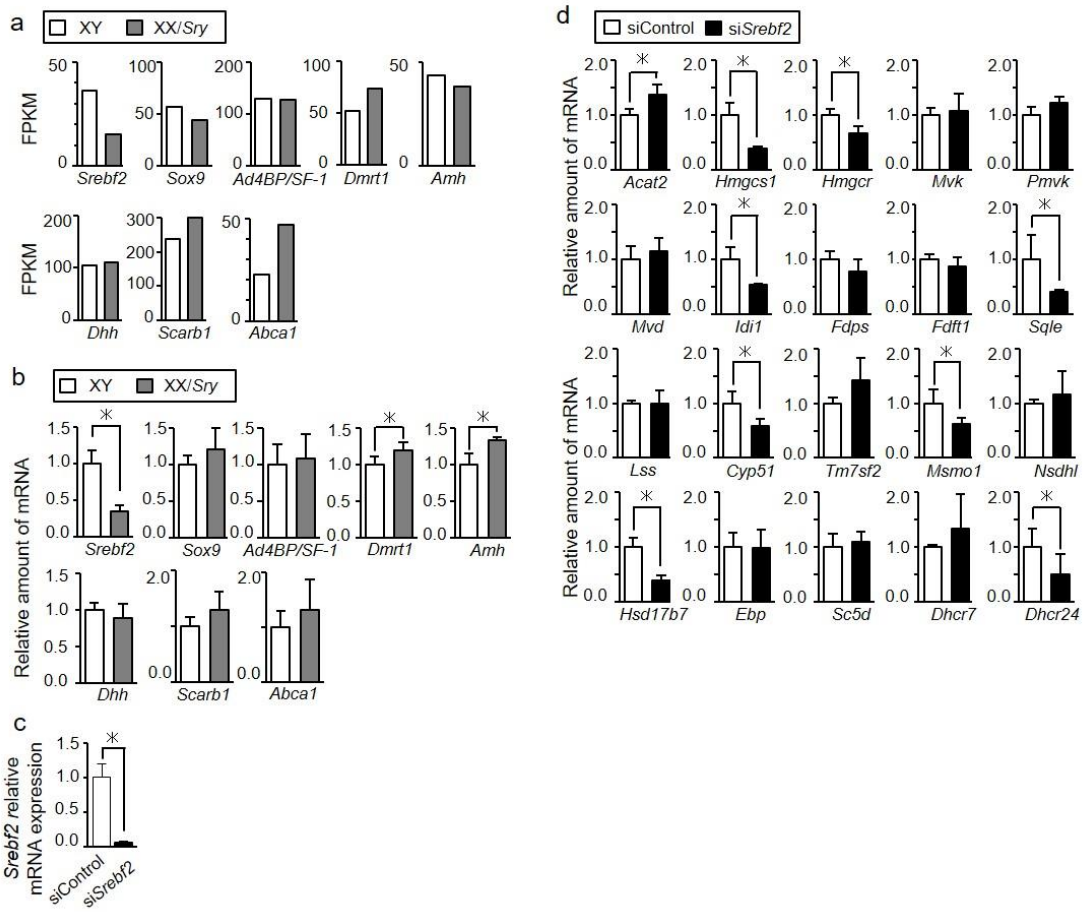

Fig. 5, Decreased expression of genes regulating cholesterol homeostasis in XX/Sry Sertoli cells

a, FPKM values of *Srebf2*, *Sox9*, *Ad4BP/Sf1*, *Dmrt1*, *Amh,* and *Dhh, Scarb1*, and *Abca1* are shown. **b,** *Srebf2*, *Sox9*, *Ad4BP/Sf1*, *Dmrt1*, *Amh*, *Dhh*, *Scarb1*, and *Abca1* were examined by qRT-PCR. The average values for the XY Sertoli cells were normalized to 1.0. **c,** XY Sertoli cells were treated with siRNA against *Srebf2* and control siRNA. The amount of *Srebf2* was determined by qRT-PCR. **d,** Expression of cholesterogenic genes in XY Sertoli cells treated with siRNA against *Srebf2* and control siRNA was examined by qRT-PCR. Average values and SDs are indicated. The average values for the siControl-treated cells were normalized to 1.0. Three biologically independent samples (n=3) were used for the qRT-PCR studies in **b**, **c**, and **d**. *$p < 0.05$.

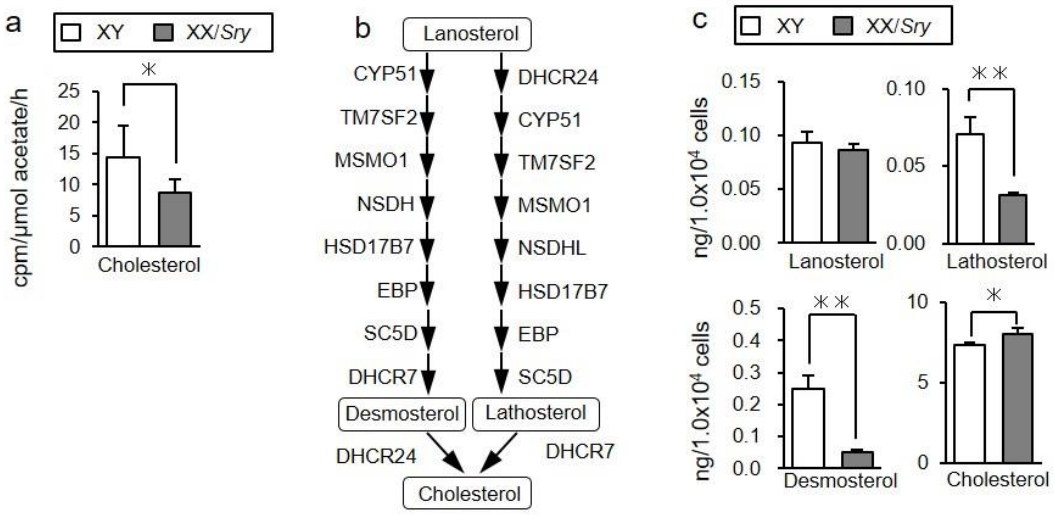

Fig. 6, Cholesterol synthesis affected in XX/Sry Sertoli cells

a, XY and XX/*Sry* Sertoli cells (1 x 10^6) were cultured in the presence of [1,2-^{14}C]-acetate and the quantities of labeled free and esterified cholesterol were determined. The studies were performed with nine biologically independent XY Sertoli cells (n = 9), and five XX/*Sry* Sertoli cells (n = 5). Error bars indicate SDs. **p* < 0.05 **b,** The late pathway for cholesterol synthesis is shown. **c,** Quantities of lanosterol, lathosterol, desmosterol, and cholesterol in XY and XX/*Sry* Sertoli cells (3 x 10^4) were determined. Average values and SDs are indicated. Four biologically independent Sertoli cell samples (n = 4) were used. **p* < 0.05; ***p* < 0.01.

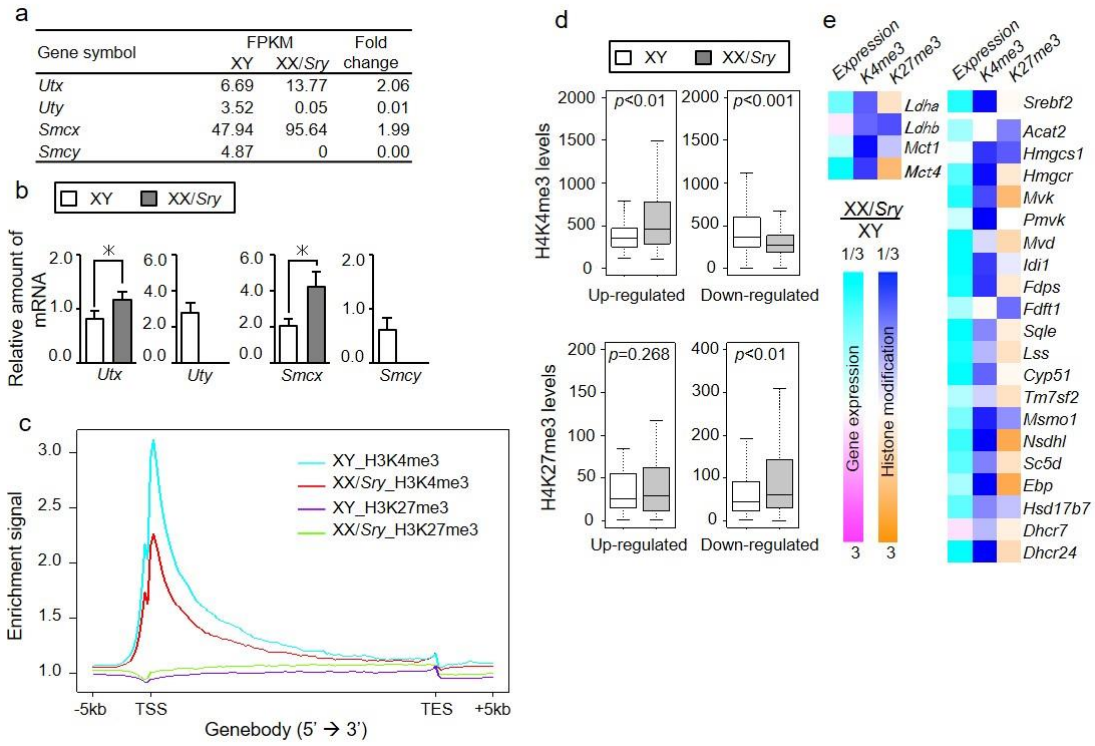

Fig. 7, Differential status of histone methylation in XY and XX/Sry Sertoli cells

a, Expression levels (FPKM) of *Utx, Uty, Smcx* and *Smcy*, revealed by mRNA sequencing for XY and XX/*Sry* Sertoli cells at P21. **b,** *Utx, Uty, Smcx* and *Smcy* expression in XY and XX/*Sry* Sertoli cells at P21 was examined by qRT-PCR. The amount of mRNA relative to Rn18s (encoding 18S ribosomal RNA) is indicated. Three biologically independent samples (n=3) were used for the qRT-PCR studies. **p* < 0.05. **c,** Global H3K4me3 and H3K27me3 deposition in XY and XX/*Sry* Sertoli cells at P21. Profiles of H3K4me3 and H3K27me3 are represented as normalized read-density. **d,** Levels of H3K4me3 and H3K27me3 for 3-fold up- or down-regulated genes in XX/*Sry* Sertoli cells. *P* values were computed using the Welch *t*-test. **e,** Fold changes in gene expression (left), H3K4me3 (middle) and H3K27me3 (right) deposition around the genes involved in lactate and cholesterol metabolism. Magenta and cyan indicate up- and down-regulated genes in XX/*Sry* Sertoli cells, respectively. Orange and blue indicate increased and decreased deposition of histone modification (H3K4me3 and H3K27me3) in XX/*Sry* Sertoli cells relative to XY Sertoli cells. Color gradients correspond to fold change; darker colors indicate a greater degree of change.

SUPPLEMENTAL TABLES

Supplemental Table S1. Oligonucleotide primers used in this study

Gene symbol	5′ Primer	3′ Primer
For genotyping PCR		
Hsp70.3prom-Sry	aaaggcgcagggcggcgagcaggccac	gccctccatgctctctagacaattcac
Ube1	tggtctggacccaaacgctgtccaca	ggcagcagccatcacataatccagatg
For qRT-PCR		
Ddx4	gcacacgttgaatacagcggggat	tgggaggaagaacagaagaacagg
Hsd3b1	caagtgtgccagccttcatct	ttcatgattctgttcctcgtgg
Sox9	tgtgacacgggacaacacatg	ggctatccacggcacacac
Cyp19a1	cccgattcggcagcaagcgt	ccagggcccgtcagagctttc
Ldha	cactgactcctgaggaagaggccc	agctcagacgagaagggtgtggtc
Ldhb	ggacaccctgtgggacatccagaa	aagcctgggctttgatctgtgagc
Mct1/Slc16a1	ccgatgtcgacgagaagccaaagc	gctctctccaggcttcacaggtca
Mct4/Slc16a3	tggttctgggcagtggtctgttca	cagcaggcagacctggaagagcta
Acat2	gtgtctgcggcaatagctaaagaa	cagccagatgctcccagaggatg
Hmgcs1	aatgaccacagtttggatgaagga	agggagtcttggcactttcttagc
Hmgcr	agccttggcagcaggacatcttgt	tcttggtgcacgttccttgaagat
Mvk	caagtaacggcagcacacggactg	tggcttgctctagacctggcttca
Pmvk	agtagtggcctcggagcagagtcg	aaagttcccaaagttgtccagacc
Mvd	gggtccagtacatcattgccactc	gcagtccatcctggcctagcagat
Idi1	cttgaaagccgagttgggaatac	ccatcagattgggccttgtagtaa
Fdps	ttcagtgtctgctacgagcctctc	ctttcacccgagccacttttttctg
Fdft1	aacatgcctgccgtcaaagctatc	gagatgacctgcttggttttgctt
Sqle	aaacttggtggagagtgtgtgacc	caacggaaaagaagtgtcgaatca
Lss	gggatcagatgtctgctagggaag	gtagctgatggcacaggacttgtt
Cyp51	cttacaggataacccagcatcagg	taggcaaaattttctccaacacaa
Tm7sf2	gggagatctcatcatggctctgg	accagcagtgcagtgaagtagagg
Msmo1	accatacgtttgctggaaaccatc	agcgcccgtataaaaaggaaccaa
Nsdhl	gacacatcttagccgctgagcac	cagaaagggattggttcatcgtt
Hsd17b7	ccacctcgggatttgggactaat	cttttccagctccagtaagacctca
Ebp	cttccgctttgtcctacagcttg	tggagtccttcgtgtagctctgtc
Sc5d	tactggattcataggggcctgcac	ggtgaaaagcatgacttgcaaacg
Dhcr7	ggtggtacctaggctggggagattg	ggagagctgcacagggtggtaca
Dhcr24	atgaggcagctggagaagtttgt	atctcccagaattcctcgcggttc
Srebf2	agctgctggagcatagcctacgg	gatggcagtagctcgctctcgtt
Ad4BP/Sf-1	aagccactctgtaggaccaagc	tgtaaatctgacgcgaaagcag
Dmrt1	gaccagtgagaagagcgggcaaac	atttggatttggggtgtggggtgc
Amh	gaacctctgccctactcggg	aagtccacggttagcaccaaa
Dhh	agcgcttccgggacctcgta	cccgctctttgcaacgctct
Scarb1	gcccacgcatgtgcaaaaacaact	aggggctgacagcagctagagttc
Abca1	gctggcaatgagtgtgccagagtt	caagacagccacaacagcagctca
Utx/Kdm6a	catcaagaaaataacaacttctgtt	aaaacaccccagtagccttcag
Uty	tgctttaatggaaaagttcattgc	gcgtaagtctcccaacacacacca
Smcx/Kdn5c	acccaaccttgtgcagtgta	gctgtagtctctttgcccgt
Smcy/Kdm5d	acagcttcctctgcccttaatccc	tgggaaacgcatacagggaatact
Rn18s	ccattcgaacgtctgccctat	gtcacccgtggtcaccatg

Supplemental Table S2. Quality data of mRNA-Seq

	Total reads	Mapped reads	Mapping rate	Number of genes detected
P1_XYSC	33,411,295	32,539,665	97.4%	16,912
P1_XX/*Sry*SC	34,885,622	33,946,217	97.3%	16,955
P21_XYSC	29,846,366	29,042,222	97.3%	17,617
P21_XX/*Sry*SC	32,676,242	31,787,030	97.3%	16,649

Supplemental Table S3. Genes up-regulated in XX/Sry Sertoli cells at P1

Gene symbol	FPKM		Fold change	Gene name
	XY	XX/*Sry*		
Sry	0.0	46.6	1,552.33	sex determining region of Chr Y
Xist	0.0	29.1	726.25	inactive X specific transcripts
Meg3	3.3	8.6	2.66	maternally expressed 3
Ccl27b	15.0	33.7	2.25	chemokine (C-C motif) ligand 27b
Cd24a	4.8	10.6	2.21	CD24a antigen
Clk1	55.9	114.9	2.05	CDC-like kinase 1
Hamp2	9.0	17.4	1.95	hepcidin antimicrobial peptide 2
Kdm6a	10.2	18.9	1.85	lysine (K)-specific demethylase 6A
Arglu1	27.1	48.5	1.79	arginine and glutamate rich 1
Neat1	8.9	15.8	1.77	nuclear paraspeckle assembly transcript 1 (non-protein coding)
Gpc3	9.2	16.3	1.76	glypican 3
Sfrs18	12.7	22.1	1.74	serine/arginine-rich splicing factor 18
Bgn	14.5	25.2	1.74	biglycan
Mgp	17.4	30.1	1.73	matrix Gla protein
Ncam1	7.2	12.3	1.72	neural cell adhesion molecule 1
Paxbp1	11.1	19.0	1.71	PAX3 and PAX7 binding protein 1
6720401G13Rik	15.9	27.1	1.70	RIKEN cDNA 6720401G13 gene
Igfbp7	8.4	14.3	1.70	insulin-like growth factor binding protein 7
Gstt1	10.4	17.7	1.69	glutathione S-transferase, theta 1
Igfbp4	12.7	21.5	1.69	insulin-like growth factor binding protein 4
Tcea2	10.7	18.0	1.68	transcription elongation factor A (SII), 2
Eif2s3x	50.6	84.9	1.68	eukaryotic translation initiation factor 2, subunit 3, structural gene X-linked
Chst11	9.1	15.3	1.68	carbohydrate sulfotransferase 11
Lime1	8.8	14.7	1.67	Lck interacting transmembrane adaptor 1
Fnbp4	18.2	30.0	1.65	formin binding protein 4
Luc7l3	18.3	30.1	1.65	LUC7-like 3 (S. cerevisiae)
Gm1821	11.9	19.5	1.64	ubiquitin pseudogene
Clk4	19.8	32.2	1.63	CDC like kinase 4
Tagln	34.2	55.6	1.63	transgelin
Smoc2	10.0	16.3	1.63	SPARC related modular calcium binding 2
Kcnt1	15.5	25.0	1.62	potassium channel, subfamily T, member 1
Gas5	12.4	19.5	1.57	growth arrest specific 5
Dcn	9.4	14.6	1.56	decorin
Acta2	16.8	26.3	1.56	actin, alpha 2, smooth muscle, aorta
Fstl1	35.8	54.2	1.51	follistatin-like 1
Srsf10	37.0	56.0	1.51	serine/arginine-rich splicing factor 10
Mfap4	14.2	21.3	1.50	microfibrillar-associated protein 4
Srsf11	36.7	55.1	1.50	serine/arginine-rich splicing factor 11

Supplemental Table S4. Genes down-regulated in XX/Sry Sertoli cells at P1

Gene symbol	FPKM		Fold change	Gene name
	XY	XX/*Sry*		
Kdm5d	6.0	0.0	0.00	lysine (K)-specific demethylase 5D
Ddx3y	22.0	0.0	0.00	DEAD (Asp-Glu-Ala-Asp) box polypeptide 3, Y-linked
Eif2s3y	25.6	0.0	0.00	eukaryotic translation initiation factor 2, subunit 3, structural gene Y-linked
Uba1y	10.9	1.0	0.09	ubiquitin-activating enzyme, Chr Y
Dpm3	24.4	3.0	0.12	dolichyl-phosphate mannosyltransferase polypeptide 3
Tppp3	14.1	3.0	0.21	tubulin polymerization-promoting protein family member 3
Gdf15	10.3	2.6	0.25	growth differentiation factor 15
Rpl36	310.4	93.9	0.30	ribosomal protein L36
Rps29	1,080.9	399.7	0.37	ribosomal protein S29
Junb	48.1	18.2	0.38	Jun-B oncogene
1500011K16Rik	8.2	3.2	0.38	RIKEN cDNA 1500011K16 gene
Tceb2	161.9	64.3	0.40	transcription elongation factor B (SIII), polypeptide 2
Smim4	15.6	6.3	0.40	small itegral membrane protein 4
Lmna	33.5	14.0	0.42	lamin A
Creb5	13.5	5.8	0.43	cAMP responsive element binding protein 5
Gm8580	11.2	4.9	0.44	ribosomal protein L29 pseudogene
Rnaseh2c	16.3	7.9	0.48	ribonuclease H2, subunit C
Gm5779	11.3	5.5	0.49	ribosomal protein, large, P0 pseudogene
Igsf9b	12.4	6.1	0.49	immunoglobulin superfamily, member 9B
Fosb	232.4	116.5	0.50	FBJ osteosarcoma oncogene B
Esyt3	12.8	6.6	0.51	extended synaptotagmin-like protein 3
Gm9833	15.5	8.2	0.53	myelin basic protein expression factor 2, repressor pseudogene
Nfatc2	12.7	6.7	0.53	nuclear factor of activated T cells, cytoplasmic, calcineurin dependent 2
Hba-a1,Hba-a2	40.3	22.1	0.55	hemoglobin alpha, adult chain 2 | hemoglobin alpha, adult chain 1
Cldn11	40.9	22.5	0.55	claudin 11
Edf1	60.1	33.5	0.56	endothelial differentiation-related factor 1
Hba-a1,Hba-a2	13.7	7.6	0.56	hemoglobin alpha, adult chain 2 | hemoglobin alpha, adult chain 1
Sssca1	21.1	11.8	0.56	Sjogren s syndrome/scleroderma autoantigen 1 homolog (human)
Col9a3	14.0	7.9	0.56	collagen, type IX, alpha 3
Rplp1	740.3	416.3	0.56	ribosomal protein, large, P1
Cidea	39.6	22.6	0.57	cell death-inducing DNA fragmentation factor, alpha subunit-like effector A
Pdlim7	59.2	34.0	0.57	PDZ and LIM domain 7
Nfix	35.5	20.4	0.57	nuclear factor I/X
Jund	40.9	23.5	0.58	Jun proto-oncogene related gene d
Fstl3	58.6	33.7	0.58	follistatin-like 3
Siva1	125.0	72.4	0.58	SIVA1, apoptosis-inducing factor
Tgm2	44.6	25.9	0.58	transglutaminase 2, C polypeptide
Pkig	48.9	28.4	0.58	protein kinase inhibitor, gamma
Pigyl	27.5	16.1	0.58	phosphatidylinositol glycan anchor biosynthesis, class Y-like
Cxx1a	19.2	11.3	0.59	CAAX box 1A
Anxa1	20.5	12.0	0.59	annexin A1
Ier3	260.5	153.9	0.59	immediate early response 3
Arid5a	14.8	8.8	0.59	AT rich interactive domain 5A (MRF1-like)
Csrnp1	60.6	36.2	0.60	cysteine-serine-rich nuclear protein 1
Ncor2	89.3	53.6	0.60	nuclear receptor co-repressor 2
Mrps12	15.3	9.2	0.60	mitochondrial ribosomal protein S12
Cdc42ep5	14.7	8.9	0.61	CDC42 effector protein (Rho GTPase binding) 5
4933409K07Rik	14.9	9.1	0.61	RIKEN cDNA 4933409K07 gene
Col9a2	28.3	17.3	0.61	collagen, type IX, alpha 2
Notch1	16.5	10.2	0.61	notch 1
Sf3b5	40.8	25.1	0.62	splicing factor 3b, subunit 5
Znhit1	14.6	9.1	0.62	zinc finger, HIT domain containing 1

(Continued on next page)

(Continued)

Gene symbol	FPKM		Fold change	Gene name
	XY	XX/*Sry*		
Beta-s	32.6	20.4	0.63	hemoglobin subunit beta-1-like
Cbln4	22.5	14.1	0.63	cerebellin 4 precursor protein
Ssbp4	35.7	22.5	0.63	single stranded DNA binding protein 4
Sfn	24.4	15.4	0.63	stratifin
Lfng	18.3	11.6	0.63	LFNG O-fucosylpeptide 3-beta-N-acetylglucosaminyltransferase
Dohh	19.1	12.1	0.63	deoxyhypusine hydroxylase/monooxygenase
Lrfn4	20.1	12.8	0.64	leucine rich repeat and fibronectin type III domain containing 4
Padi2	35.6	22.8	0.64	peptidyl arginine deiminase, type II
Fau	681.7	438.8	0.64	Finkel-Biskis-Reilly murine sarcoma virus (FBR-MuSV) ubiquitously expressed (fox derived)
Rps21	800.7	515.8	0.64	ribosomal protein S21
2700094K13Rik	51.8	33.4	0.64	RIKEN cDNA 2700094K13 gene
Bola2	57.2	36.9	0.65	bolA-like 2 (E. coli)
Sh3bp4	30.7	19.8	0.65	SH3-domain binding protein 4
Psmg4	20.5	13.2	0.65	proteasome (prosome, macropain) assembly chaperone 4
Pdlim1	16.0	10.3	0.65	PDZ and LIM domain 1 (elfin)
Cystm1	36.0	23.3	0.65	cysteine-rich transmembrane module containing 1
Fabp3	63.7	41.3	0.65	fatty acid binding protein 3, muscle and heart
Klf3	20.6	13.4	0.65	Kruppel-like factor 3 (basic)
Nr1d1	23.5	15.3	0.65	nuclear receptor subfamily 1, group D, member 1
Ddah2	22.5	14.7	0.65	dimethylarginine dimethylaminohydrolase 2
Sox9	87.4	57.1	0.65	SRY-box containing gene 9
Hexim1	36.2	23.7	0.65	hexamethylene bis-acetamide inducible 1
Arl10	19.4	12.7	0.66	ADP-ribosylation factor-like 10
Dbn1	42.8	28.2	0.66	drebrin 1
Uqcr10	124.5	82.0	0.66	ubiquinol-cytochrome c reductase, complex III subunit X
Arid5b	36.7	24.3	0.66	AT rich interactive domain 5B (MRF1-like)
Myc	17.2	11.4	0.66	myelocytomatosis oncogene
Polr2l	47.4	31.4	0.66	polymerase (RNA) II (DNA directed) polypeptide L
Crym	17.0	11.3	0.66	crystallin, mu
Cxx1b	19.7	13.1	0.66	CAAX box 1B
Galk1	27.2	18.0	0.66	galactokinase 1
S100a10	192.8	128.3	0.66	S100 calcium binding protein A10 (calpactin)
Vps37b	35.7	23.8	0.66	vacuolar protein sorting 37B (yeast)
Ctgf	192.5	128.1	0.66	connective tissue growth factor

Supplemental Table S5. GO and KEGG pathway analysis using genes up-regulated in XX/Sry Sertoli cells at P21

ID	Term	Fold enrichment	P-value
GO:0050840	extracellular matrix binding	13.05	1.1.E-05
GO:0005520	insulin-like growth factor binding	10.60	1.1.E-03
GO:0001755	neural crest cell migration	10.40	1.2.E-03
GO:0014032	neural crest cell development	8.70	5.6.E-04
GO:0014033	neural crest cell differentiation	8.70	5.6.E-04
GO:0048762	mesenchymal cell differentiation	6.84	5.1.E-04
GO:0060485	mesenchyme development	6.70	5.7.E-04
GO:0045785	positive regulation of cell adhesion	6.68	1.9.E-03
GO:0040017	positive regulation of locomotion	6.52	2.1.E-03
GO:0019838	growth factor binding	6.48	2.1.E-05
GO:0030335	positive regulation of cell migration	6.47	7.1.E-03
GO:0014031	mesenchymal cell development	6.11	2.8.E-03
GO:0030027	lamellipodium	6.06	3.3.E-04
GO:0030334	regulation of cell migration	5.20	1.2.E-04
GO:0031589	cell-substrate adhesion	5.04	6.5.E-03
GO:0040012	regulation of locomotion	4.78	9.8.E-05
GO:0030155	regulation of cell adhesion	4.58	7.6.E-04
GO:0051270	regulation of cell motion	4.47	3.9.E-04
GO:0051216	cartilage development	4.29	5.7.E-03
GO:0031252	cell leading edge	4.26	5.5.E-04
GO:0043405	regulation of MAP kinase activity	3.99	8.1.E-03
GO:0008201	heparin binding	3.93	8.6.E-03
GO:0060348	bone development	3.65	3.3.E-03
GO:0001503	ossification	3.61	6.7.E-03
GO:0048514	blood vessel morphogenesis	3.38	2.6.E-04
GO:0007169	transmembrane receptor protein tyrosine kinase signaling pathway	3.24	7.0.E-04
GO:0008509	anion transmembrane transporter activity	3.23	6.8.E-03
GO:0007167	enzyme linked receptor protein signaling pathway	3.15	6.0.E-05
GO:0001944	vasculature development	3.06	2.4.E-04
GO:0015629	actin cytoskeleton	3.03	1.2.E-03
GO:0001568	blood vessel development	2.94	6.1.E-04
GO:0035239	tube morphogenesis	2.80	9.6.E-03
GO:0001501	skeletal system development	2.69	9.5.E-04
GO:0051094	positive regulation of developmental process	2.68	5.3.E-03
GO:0044057	regulation of system process	2.62	9.6.E-03
GO:0035295	tube development	2.36	9.5.E-03
GO:0031012	extracellular matrix	2.32	5.4.E-03
GO:0007155	cell adhesion	2.30	1.2.E-04
GO:0022610	biological adhesion	2.30	1.2.E-04
GO:0045944	positive regulation of transcription from RNA polymerase II promoter	2.27	3.5.E-03
GO:0005578	proteinaceous extracellular matrix	2.25	9.7.E-03
GO:0008092	cytoskeletal protein binding	2.14	3.5.E-03
GO:0045893	positive regulation of transcription, DNA-dependent	2.07	6.4.E-03
GO:0051254	positive regulation of RNA metabolic process	2.06	6.9.E-03
GO:0042127	regulation of cell proliferation	2.05	2.0.E-03
GO:0006357	regulation of transcription from RNA polymerase II promoter	2.02	1.1.E-03
GO:0005509	calcium ion binding	2.00	1.1.E-04
GO:0044421	extracellular region part	1.85	1.6.E-03
GO:0005576	extracellular region	1.42	8.8.E-03
GO:0043167	ion binding	1.27	2.9.E-03
GO:0046872	metal ion binding	1.26	4.3.E-03
GO:0043169	cation binding	1.25	5.8.E-03
mmu04512	ECM-receptor interaction	4.32	2.3.E-03
mmu04510	Focal adhesion	2.94	1.3.E-03
mmu04810	Regulation of actin cytoskeleton	2.89	9.4.E-04

Supplemental Table S6. GO and KEGG pathway analysis using genes down-regulated in XX/Sry Sertoli cells at P21

ID	Term	Fold enrichment	P-value
GO:0033391	chromatoid body	26.7	4.2.E-07
GO:0034587	piRNA metabolic process	22.0	4.5.E-04
GO:0004459	L-lactate dehydrogenase activity	20.2	7.8.E-03
GO:0043186	P granule	19.0	6.2.E-05
GO:0060293	germ plasm	19.0	6.2.E-05
GO:0045495	pole plasm	19.0	6.2.E-05
GO:0004029	aldehyde dehydrogenase (NAD) activity	13.5	2.5.E-03
GO:0030291	protein serine/threonine kinase inhibitor activity	12.0	3.6.E-03
GO:0006695	cholesterol biosynthetic process	12.0	5.3.E-08
GO:0005844	polysome	11.4	1.1.E-04
GO:0016126	sterol biosynthetic process	11.0	3.8.E-09
GO:0005665	DNA-directed RNA polymerase II, core complex	9.7	6.9.E-03
GO:0008299	isoprenoid biosynthetic process	8.8	1.0.E-04
GO:0007339	binding of sperm to zona pellucida	8.1	2.8.E-03
GO:0030374	ligand-dependent nuclear receptor transcription coactivator activity	7.7	8.5.E-04
GO:0035036	sperm-egg recognition	7.6	3.5.E-03
GO:0006367	transcription initiation from RNA polymerase II promoter	7.6	3.5.E-03
GO:0001673	male germ cell nucleus	7.4	3.9.E-03
GO:0009988	cell-cell recognition	6.9	5.2.E-03
GO:0000795	synaptonemal complex	6.7	5.8.E-03
GO:0043073	germ cell nucleus	6.1	8.3.E-03
GO:0007051	spindle organization	5.9	3.0.E-03
GO:0000794	condensed nuclear chromosome	5.7	1.4.E-04
GO:0016620	oxidoreductase activity, acting on the aldehyde or oxo group of donors, NAD or NADP as acceptor	5.6	3.9.E-03
GO:0051321	meiotic cell cycle	5.5	2.0.E-08
GO:0006694	steroid biosynthetic process	5.4	1.4.E-06
GO:0051327	M phase of meiotic cell cycle	5.3	9.2.E-08
GO:0007126	meiosis	5.3	9.2.E-08
GO:0044450	microtubule organizing center part	5.2	5.5.E-03
GO:0006720	isoprenoid metabolic process	5.1	3.4.E-04
GO:0016125	sterol metabolic process	5.0	3.5.E-06
GO:0030176	integral to endoplasmic reticulum membrane	4.8	7.2.E-03
GO:0035257	nuclear hormone receptor binding	4.8	7.8.E-03
GO:0008203	cholesterol metabolic process	4.7	4.0.E-05
GO:0007127	meiosis I	4.7	8.1.E-03
GO:0034062	RNA polymerase activity	4.6	8.8.E-03
GO:0003899	DNA-directed RNA polymerase activity	4.6	8.8.E-03
GO:0019887	protein kinase regulator activity	4.6	2.9.E-04
GO:0006366	transcription from RNA polymerase II promoter	4.5	6.8.E-05
GO:0006096	glycolysis	4.4	4.8.E-03
GO:0019861	flagellum	4.4	9.4.E-04
GO:0016591	DNA-directed RNA polymerase II, holoenzyme	4.3	1.1.E-03
GO:0006007	glucose catabolic process	4.2	2.6.E-03
GO:0019320	hexose catabolic process	4.2	2.6.E-03
GO:0046365	monosaccharide catabolic process	4.1	3.2.E-03
GO:0003729	mRNA binding	4.0	3.6.E-03
GO:0007283	spermatogenesis	4.0	2.2.E-12
GO:0048232	male gamete generation	4.0	2.2.E-12
GO:0007286	spermatid development	3.7	5.3.E-03
GO:0019207	kinase regulator activity	3.7	1.4.E-03
GO:0044275	cellular carbohydrate catabolic process	3.7	5.8.E-03
GO:0007281	germ cell development	3.5	2.9.E-04
GO:0048515	spermatid differentiation	3.5	7.6.E-03
GO:0001666	response to hypoxia	3.4	8.3.E-03
GO:0046164	alcohol catabolic process	3.4	9.0.E-03

(Continued on next page)

(Continued)

GO:0070482	response to oxygen levels	3.4	9.0.E-03
GO:0048610	reproductive cellular process	3.3	4.7.E-06
GO:0007276	gamete generation	3.2	2.9.E-10
GO:0000279	M phase	3.2	1.1.E-08
GO:0048609	reproductive process in a multicellular organism	3.2	7.3.E-12
GO:0032504	multicellular organism reproduction	3.2	7.3.E-12
GO:0019953	sexual reproduction	3.1	5.0.E-11
GO:0006417	regulation of translation	3.0	3.4.E-03
GO:0022403	cell cycle phase	3.0	1.0.E-08
GO:0022402	cell cycle process	3.0	3.1.E-10
GO:0000793	condensed chromosome	3.0	2.2.E-03
GO:0000228	nuclear chromosome	2.9	1.9.E-03
GO:0010608	posttranscriptional regulation of gene expression	2.8	9.8.E-04
GO:0006006	glucose metabolic process	2.8	1.7.E-03
GO:0008202	steroid metabolic process	2.7	7.7.E-04
GO:0006351	transcription, DNA-dependent	2.7	4.8.E-03
GO:0005819	spindle	2.7	7.6.E-03
GO:0030005	cellular di-, tri-valent inorganic cation homeostasis	2.7	3.5.E-03
GO:0032774	RNA biosynthetic process	2.6	6.1.E-03
GO:0019318	hexose metabolic process	2.6	1.3.E-03
GO:0005815	microtubule organizing center	2.5	7.4.E-04
GO:0030003	cellular cation homeostasis	2.5	3.6.E-03
GO:0007049	cell cycle	2.5	3.8.E-10
GO:0003006	reproductive developmental process	2.5	9.5.E-05
GO:0044092	negative regulation of molecular function	2.5	8.6.E-03
GO:0005813	centrosome	2.5	2.7.E-03
GO:0055066	di-, tri-valent inorganic cation homeostasis	2.4	6.9.E-03
GO:0008610	lipid biosynthetic process	2.4	1.1.E-04
GO:0000278	mitotic cell cycle	2.4	5.9.E-04
GO:0042175	nuclear envelope-endoplasmic reticulum network	2.3	7.1.E-03
GO:0005996	monosaccharide metabolic process	2.3	4.1.E-03
GO:0055080	cation homeostasis	2.2	7.2.E-03
GO:0005874	microtubule	2.2	1.7.E-03
GO:0006873	cellular ion homeostasis	2.1	3.2.E-03
GO:0015630	microtubule cytoskeleton	2.1	7.8.E-05
GO:0055082	cellular chemical homeostasis	2.1	4.2.E-03
GO:0030529	ribonucleoprotein complex	2.0	1.3.E-04
GO:0050801	ion homeostasis	2.0	5.1.E-03
GO:0019725	cellular homeostasis	1.8	7.1.E-03
GO:0005694	chromosome	1.8	4.2.E-03
GO:0048878	chemical homeostasis	1.8	7.4.E-03
GO:0055114	oxidation reduction	1.6	2.5.E-03
GO:0044430	cytoskeletal part	1.6	1.2.E-03
GO:0043228	non-membrane-bounded organelle	1.5	2.7.E-06
GO:0043232	intracellular non-membrane-bounded organelle	1.5	2.7.E-06
GO:0005783	endoplasmic reticulum	1.5	9.2.E-03
GO:0005856	cytoskeleton	1.4	7.0.E-03
GO:0070013	intracellular organelle lumen	1.4	8.5.E-03
GO:0043233	organelle lumen	1.4	9.0.E-03
GO:0030554	adenyl nucleotide binding	1.3	6.9.E-03
GO:0001882	nucleoside binding	1.3	6.8.E-03
GO:0001883	purine nucleoside binding	1.3	8.6.E-03
GO:0017076	purine nucleotide binding	1.3	6.6.E-03
mmu00900	Terpenoid backbone biosynthesis	11.1	1.2.E-04
mmu00100	Steroid biosynthesis	9.1	3.4.E-04
mmu00640	Propanoate metabolism	6.0	8.3.E-04
mmu03020	RNA polymerase	5.7	3.3.E-03
mmu00620	Pyruvate metabolism	4.4	4.4.E-03
mmu00010	Glycolysis / Gluconeogenesis	3.8	1.1.E-03